Preparation and Activation of Complexes of the Type $[((mesityl)NCH_2CH_2)_2NX]ZrMe_2$ (X = H, Me) with $[Ph_3C][B(C_6F_5)_4]$ or $[PhNMe_2H][B(C_6F_5)_4]$

Richard R. Schrock,* Arturo L. Casado, Jonathan T. Goodman, Lan-Chang Liang, Peter J. Bonitatebus, Jr., and William M. Davis

Department of Chemistry, Massachusetts Institute of Technology, 77 Massachusetts Avenue, Cambridge, Massachusetts 02139

Received June 13, 2000

The zirconium dimethyl complexes $[N_2NX]ZrMe_2$ (N_2NX = $[(MesNCH_2CH_2)_2NX]$; Mes = mesityl; X = H (**1a**), Me (**1b**)), have "mer" structures in the solid state in which the amido nitrogens occupy "axial" positions in a trigonal bipyramid. The reaction of **1b** with 1 equiv of $[Ph_3C][B(C_6F_5)_4]$ followed by addition of diethyl ether yielded the ether adduct $\{[N_2NMe]ZrMe(Et_2O)\}^+$ (with $[B(C_6F_5)_4]^-$ as the anion), an X-ray study of which revealed it to be a *fac* trigonal-bipyramidal species in which the diethyl ether is coordinated in an apical position. The reaction of **1b** with 1 equiv of $[PhNMe_2H][B(C_6F_5)_4]$ led to $\{[N_2NMe]ZrMe(NMe_2Ph)\}[B(C_6F_5)_4]$, solution NMR studies of which suggest a structure analogous to that of $\{[N_2NMe]ZrMe(Et_2O)\}^+$. Heating solutions of $\{[N_2NMe]ZrMe(NMe_2Ph)\}[B(C_6F_5)_4]$ led to C−H activation in one mesityl *o*-methyl group and formation of methane. The reaction of **1b** with 0.5 equiv of $[Ph_3C][B(C_6F_5)_4]$ yielded $[\{[N_2NMe]ZrMe\}_2(\mu\text{-Me})][B(C_6F_5)_4]$ (**5b**), an X-ray diffraction study of which revealed an almost linear (167.4°) methyl bridge linking two distorted TBP moieties through the apical positions (average Zr−C(bridge) = 2.48 Å, average Zr−C(terminal) = 2.24 Å). The equatorial methyl groups in **5b** exchange readily between Zr centers, while the bridging methyl group and the equatorial methyl groups exchange relatively slowly on the NMR time scale, but still rapidly on the chemical time scale. Exchange of free $[N_2NMe]ZrMe_2$ with the $[N_2NMe]ZrMe_2$ fragment in **5b** is also facile on the chemical time scale. The reaction of **1b** with 1.0 equiv or more of $[Ph_3C][B(C_6F_5)_4]$ led to formation of a cationic species (**6b**), two forms of which could be observed at low temperature. Activation of **1a** with $[Ph_3C][B(C_6F_5)_4]$ yielded only one cationic form of **6a** at low temperatures. Exchange of methyl groups between **6a** and **6b** is slow on the chemical time scale. All evidence is consistent with the observation of different ion pairs of **6b** at low temperatures.

Introduction

Dialkylzirconium(IV) complexes that contain diamido/donor ligands, e.g., $[(t\text{-Bu-N-}o\text{-}C_6H_4)_2O]^{2-}$,[1−3] $[(MesNCH_2CH_2)_2NR]^{2-}$ (Mes = mesityl; R = H, Me),[4] and others,[5−13] have been prepared and studied recently in our laboratory. They are members of a growing class of group 4 metal diamido complexes that are being explored for early-transition-metal chemistry, often with the goal of preparing new olefin polymerization catalysts.[14−46] We have found that dimethyl

(1) Baumann, R.; Schrock, R. R. *J. Organomet. Chem.* **1998**, *557*, 69.
(2) Schrock, R. R.; Baumann, R.; Reid, S. M.; Goodman, J. T.; Stumpf, R.; Davis, W. M. *Organometallics* **1999**, *18*, 3649.
(3) Baumann, R.; Davis, W. M.; Schrock, R. R. *J. Am. Chem. Soc.* **1997**, *119*, 9, 3830.
(4) Liang, L.-C.; Schrock, R. R.; Davis, W. M.; McConville, D. H. *J. Am. Chem. Soc.* **1999**, *120*, 5797.
(5) Schrock, R. R.; Schattenmann, F.; Aizenberg, M.; Davis, W. M. *Chem. Commun.* **1998**, 199.
(6) Aizenberg, M.; Turculet, L.; Davis, W. M.; Schattenmann, F.; Schrock, R. R. *Organometallics* **1998**, *17*, 4795.
(7) Schattenmann, F.; Schrock, R. R.; Davis, W. M. *Organometallics* **1998**, *17*, 989.
(8) Schrock, R. R.; Lee, J.; Liang, L.-C.; Davis, W. M. *Inorg. Chim. Acta* **1998**, *270*, 353.
(9) Schrock, R. R.; Seidel, S. W.; Schrodi, Y.; Davis, W. M. *Organometallics* **1999**, *118*, 428.
(10) Graf, D. D.; Schrock, R. R.; Davis, W. M.; Stumpf, R. *Organometallics* **1999**, *18*, 843.
(11) Flores, M. A.; Manzoni, M.; Baumann, R.; Davis, W. M.; Schrock, R. R. *Organometallics* **1999**, *18*, 3220.
(12) Baumann, R.; Stumpf, R.; Davis, W. M.; Liang, L.-C.; Schrock, R. *J. Am. Chem. Soc.* **1999**, *121*, 7822.
(13) Schrock, R. R.; Liang, L.-C.; Baumann, R.; Davis, W. M. *J. Organomet. Chem.* **1999**, *591*, 163.
(14) Scollard, J. D.; McConville, D. H.; Vittal, J. J. *Organometallics* **1995**, *14*, 5478.
(15) Scollard, J. D.; McConville, D. H. *J. Am. Chem. Soc.* **1996**, *118*, 10008.
(16) Scollard, J. D.; McConville, D. H.; Payne, N. C.; Vittal, J. J. *Macromolecules* **1996**, *29*, 5241.
(17) Scollard, J. D.; McConville, D. H.; Rettig, S. J. *Organometallics* **1997**, *16*, 1810.
(18) Scollard, J. D.; McConville, D. H.; Vittal, J. J. *Organometallics* **1997**, *16*, 4415.
(19) Scollard, J. D.; McConville, D. H.; Vittal, J. J.; Payne, N. C. *J. Mol. Catal. A* **1998**, *128*, 201.
(20) Guérin, F.; McConville, D. H.; Payne, N. C. *Organometallics* **1996**, *15*, 5085.
(21) Guérin, F.; McConville, D. H.; Vittal, J. J. *Organometallics* **1996**, *15*, 5586.
(22) Guérin, F.; McConville, D. H.; Vittal, J. J. *Organometallics* **1997**, *16*, 1491.
(23) Guérin, F.; Del Vecchio, G.; McConville, D. H. *Polyhedron* **1998**, *17*, 917.
(24) Guérin, F.; McConville, D. H.; Vittal, J. J.; Yap, G. A. P. *Organometallics* **1998**, *17*, 5172.

10.1021/om0004996 CCC: $19.00
Publication on Web 11/11/2000

complexes that contain a diamido/donor ligand in which oxygen is the central donor can be activated with $[PhNMe_2H][B(C_6F_5)_4]$ or $[Ph_3C][B(C_6F_5)_4]$ to give cationic complexes that will polymerize 1-hexene efficiently. In the case of the $[(t\text{-Bu-N-}o\text{-}C_6H_4)_2O]^{2-}$ system, the polymerization occurs in a living fashion below ~10 °C via 1,2-insertions into the Zr−C bond, as shown by ^{13}C labeling[1] and kinetic[47] studies. Ligands that contain a central amine donor, $[(MesNCH_2CH_2)_2NR]^{2-}$,[4] also show significant promise for 1-hexene polymerization, although in preliminary studies they are not as well-behaved as complexes that contain the $[(t\text{-Bu-N-}o\text{-}C_6H_4)_2O]^{2-}$ ligand in terms of living characteristics for 1-hexene polymerization. The $[(MesNCH_2CH_2)_2NR]ZrMe_2$ systems are of special interest, because $[(MesNCH_2CH_2)_2NR]ZrMe_2$ can be activated with MAO in chlorobenzene, while the attempted activation of $[(t\text{-Bu-N-}o\text{-}C_6H_4)_2O]ZrMe_2$ under similar conditions did not lead to an active polymerization catalyst.[47] Therefore, we set out to explore in detail the nature of the species formed upon activation of $[(MesNCH_2CH_2)_2NR]ZrMe_2$ species (R = H, Me) with $[PhNMe_2H][B(C_6F_5)_4]$ or $[Ph_3C][B(C_6F_5)_4]$. Our initial efforts are reported here. Further elaboration of these initial findings and the use of activated complexes for the polymerization of olefins will be reported in due course.

Results

Synthesis of $[N_2NX]Zr(CH_3)_2$ ($[N_2NX] = [(MesNCH_2CH_2)_2NX]^{2-}$; X = H (1a), CH_3 (1b); Mes = Mesityl). As reported in a preliminary communication,[4] $(MesNHCH_2CH_2)_2NH$ ($H_2[N_2NH]$) can be prepared by the palladium-catalyzed reaction[48−51] between 2 equiv of mesityl bromide and diethylenetriamine. A reliable method of preparing dimethyl complexes that contain the $[N_2NH]^{2-}$ ligand involves the reaction of $H_2[N_2NH]$ with $Zr(NMe_2)_4$ to yield $[N_2NH]Zr(NMe_2)_2$. Treatment of $[N_2NH]Zr(NMe_2)_2$ with Me_3SiCl yields $[N_2NH]ZrCl_2$, which upon treatment with CH_3MgX (X = Cl, Br, I) affords $[N_2NH]ZrMe_2$. Treatment of $[N_2NH]ZrMe_2$ (**1a**) with methyllithium followed by methyl iodide was found to yield $[N_2NMe]ZrMe_2$ (**1b**).[4] It is also possible to prepare either **1a** or **1b** in one pot directly from $H_2[N_2NH]$ and $ZrCl_4$ via methylation of the initial adduct, "$\{H_2[N_2NH]\}ZrCl_4$", with 4 equiv of CH_3MgI (to give **1a**) or with 5 equiv of methyllithium followed by methyl iodide (to give **1b**). Alternatively, $H_2[N_2NMe]$ can be prepared directly from $H_2[N_2NH]$ in ~80% yield by treating it with MeI in acetonitrile at room temperature in the presence of potassium carbonate (eq 1). $[N_2NMe]ZrMe_2$ is then prepared by methods analogous to those described for the $H_2[N_2NH]$ system.

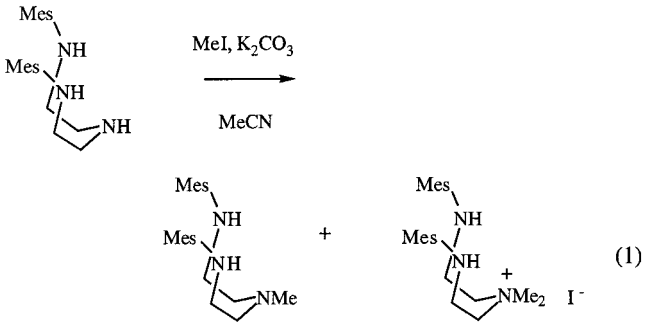

(1)

Addition of 1 equiv of $LiCH_3$ to $[N_2NH]Zr(^{13}CH_3)_2$ followed by $^{13}CH_3I$ yielded $[N_2NMe]ZrMe_2$, in which two-thirds of the methyl groups on Zr are ^{13}C-labeled, while the methyl group on the central nitrogen is completely ^{13}C-labeled (Scheme 1). This conclusion follows from observation of two 1:1:1 patterns in the ^1H NMR spectrum for the two inequivalent zirconium methyl resonances (J_{CH} = 114, 114 Hz) and a doublet resonance for the methyl group on the central nitrogen (J_{CH} = 136 Hz). We conclude that the two labeled methyl groups in $[N_2NH]Zr(^{13}CH_3)_2$ statistically scramble with the methyl group in $LiCH_3$ before methane is evolved. Possible mechanisms for scrambling of the labeled and unlabeled methyl groups include fast axial/equatorial exchange within a neutral dimethyl species, methyl scrambling via a nonspecific Zr/Li methyl exchange, or methyl scrambling via a "turnstile" mechanism within pseudooctahedral "$\{[N_2NH]ZrMe_3\}^-$". Although the precise mechanism of methane formation is not known, it seems plausible that a $[N_2NLi]ZrMe_2$ species is formed and that it reacts cleanly with $^{13}CH_3I$ to yield the observed product. In general, under no circumstances have we obtained evidence for any reaction at the central nitrogen atom or at the methyl group on the central nitrogen in $[N_2NMe]ZrMe_2$, at least none that leads to any identifiable change. Therefore, the reso-

(25) Aoyagi, K.; Gantzel, P. K.; Kalai, K.; Tilley, T. D. *Organometallics* **1996**, *15*, 923.
(26) Warren, T. H.; Schrock, R. R.; Davis, W. M. *Organometallics* **1996**, *15*, 562.
(27) Warren, T. H.; Schrock, R. R.; Davis, W. M. *Organometallics* **1998**, *17*, 308.
(28) Clark, H. C. S.; Cloke, F. G. N.; Hitchcock, P. B.; Love, J. B.; Wainwright, A. P. *J. Organomet. Chem.* **1995**, *501*, 333.
(29) Cloke, F. G. N.; Hitchcock, P. B.; Love, J. B. *J. Chem. Soc., Dalton Trans.* **1995**, 25.
(30) Cloke, F. G. N.; Geldbach, T. J.; Hitchcock, P. B.; Love, J. B. *J. Organomet. Chem.* **1996**, *506*, 343.
(31) Herrmann, W. A.; Denk, M.; Albach, R. W.; Behm, J.; Herdtweck, E. *Chem. Ber.* **1991**, *124*, 683.
(32) Horton, A. D.; de With, J. *Chem. Commun.* **1996**, 1375.
(33) Horton, A. D.; de With, J.; van der Linden, A. J.; van de Weg, H. *Organometallics* **1996**, *15*, 2672.
(34) Friedrich, S.; Gade, L. H.; Edwards, A. J.; Mcpartlin, M. *J. Chem. Soc., Dalton Trans.* **1993**, 2861.
(35) Friedrich, S.; Gade, L. H.; Scowen, I. J.; McPartlin, M. *Angew. Chem., Int. Ed. Engl.* **1996**, *35*, 1338.
(36) Jeon, Y.-M.; Park, S. J.; Heo, J.; Kim, K. *Organometallics* **1998**, *17*, 3161.
(37) Male, N. A. H.; Thornton-Pett, M.; Bochmann, M. *J. Chem. Soc., Dalton Trans.* **1997**, 2487.
(38) Tinkler, S.; Deeth, R. J.; Duncalf, D. J.; McCamley, A. *Chem. Commun.* **1996**, 2623.
(39) Tsuie, B.; Swenson, D. C.; Jordan, R. F.; Petersen, J. L. *Organometallics* **1997**, *16*, 1392.
(40) Kempe, R. *Angew. Chem., Int. Ed.* **2000**, *39*, 468.
(41) Lee, C. H.; La, Y.-H.; Park, S. J.; Park, J. W. *Organometallics* **1998**, *17*, 3648.
(42) Lee, C. H.; La, Y.-H.; Park, J. W. *Organometallics* **2000**, *19*, 344.
(43) Ziniuk, Z.; Goldberg, I.; Kol, M. *Inorg. Chem. Commun.* **1999**, *2*, 549.
(44) Armistead, L. T.; White, P. S.; Gagne, M. R. *Organometallics* **1998**, *17*, 216.
(45) Love, J. B.; Clark, H. C. S.; Cloke, F. G. N.; Green, J. C.; Hitchcock, P. B. *J. Am. Chem. Soc.* **1999**, *121*, 6843.
(46) Fryzuk, M. D.; Love, J. B.; Rettig, S. J. *Organometallics* **1998**, *17*, 846.
(47) Goodman, J. T. Unpublished observations.
(48) Hartwig, J. F. *Angew. Chem., Int. Ed. Engl.* **1998**, *37*, 2046.
(49) Wolfe, J. P.; Wagaw, S.; Buchwald, S. L. *J. Am. Chem. Soc.* **1996**, *118*, 7215.
(50) Wolfe, J. P.; Wagaw, S.; Marcoux, J. F.; Buchwald, S. L. *Acc. Chem. Res.* **1998**, *31*, 805.
(51) Wolfe, J. P.; Buchwald, S. L. *J. Org. Chem.* **2000**, *65*, 1144.

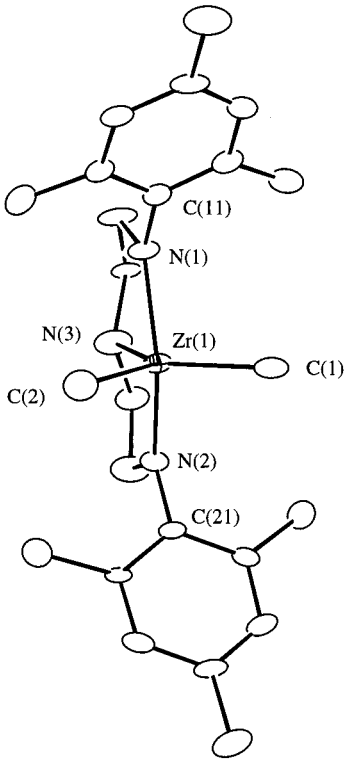

Figure 1. ORTEP drawing of the structure of [N_2NH]-$ZrMe_2$ (**1a**).

Scheme 1

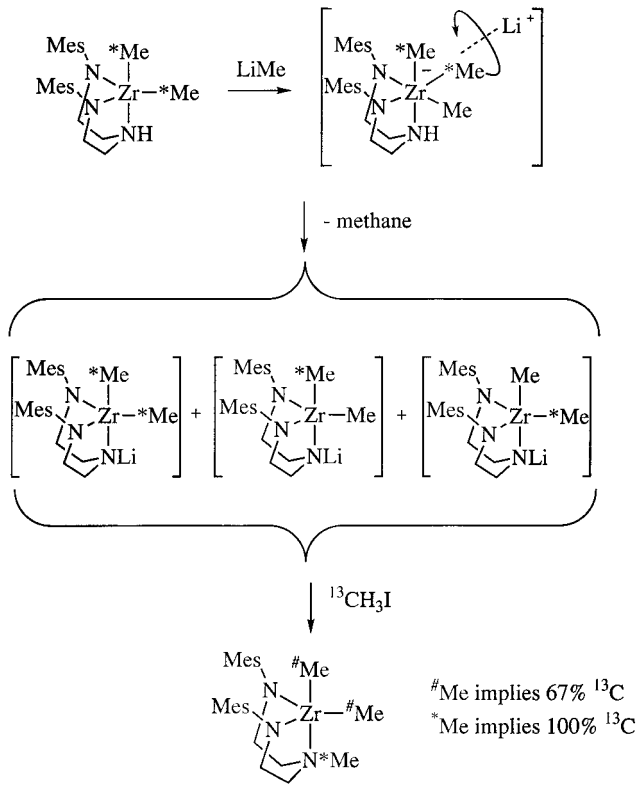

nance for the methyl group on the central nitrogen is a convenient marker and/or internal standard in ^{1}H and ^{13}C NMR studies.

The structures of **1a** and **1b** are shown in Figures 1 and 2. (See Table 1 for crystallographic details and Table 2 for selected bond distances and angles.) The coordination geometry about each Zr is a distorted

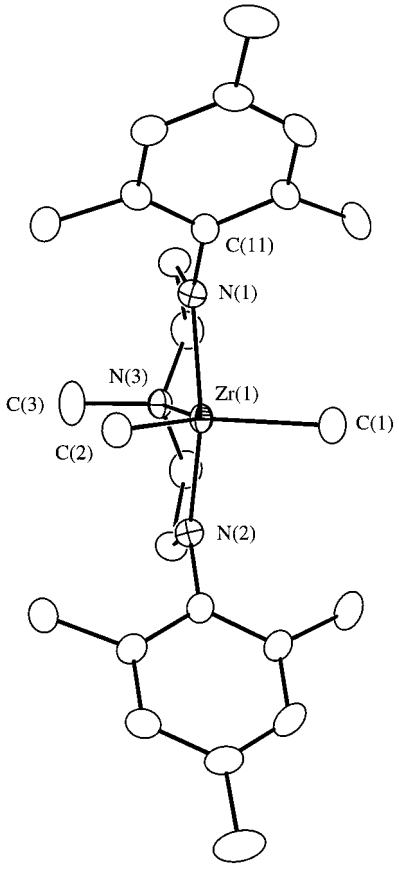

Figure 2. ORTEP drawing of the structure of [N_2NMe]-$ZrMe_2$ (**1b**).

trigonal bipyramid with "axial" amido nitrogen atoms and "equatorial" methyl groups, which we call the *mer* form. In both structures the three nitrogen atoms lie in a plane that approximately bisects the C(1)−Zr−C(2) angle. The donor amine nitrogen atom is approximately tetrahedral in each compound (C−N−C = 109, 109, and 112° for **1b**), although the $C_{arm}-N_{donor}-C_{arm}$ angle in **1a** is slightly larger (116.5(7)°) than it is in **1b** (112.3(6)°). The Zr−N_{amine}, Zr−N_{amido}, and Zr−Me bond lengths and C−Zr−C, N−Zr−N, and Zr−N−C bond angles are all typical of diamido/N_{donor} complexes having this "*mer*" geometry.[2] The two amido nitrogens in **1b** are bent only slightly away from the side of the molecule that contains C(3), as judged by the difference between the N(1)−Zr−C(1) and N(1)−Zr−C(2) angles (∼1.3°; Table 2). The *mer* geometry in compounds of this type is clearly shown by the angle between the N(1)−Zr−N(3) and N(2)−Zr−N(3) planes: 174° in **1a** and 178° in **1b**. In comparison, the angle between the N(1)−Zr−N(3) and N(2)−Zr−N(3) planes in a facially coordinated ligand is only ∼130°. (See below for an example.)

NMR spectra reveal two inequivalent ZrMe groups with proton resonances at 0.24 and 0.07 ppm in **1a** and 0.26 and 0.23 ppm in **1b** (C_6D_6, 20 °C). In ^{13}C NMR spectra, the ZrMe resonances are found at 42.45 and 39.63 ppm in **1a** and 43.31 and 40.62 ppm in **1b**. The chemical shifts for the methyl groups are somewhat temperature-dependent, but we cannot say with certainty on the basis of the chemical shift or temperature dependence what the conformation is of each species in solution. In **1b** the NMe resonances are found at 2.01

Table 1. Crystal Data and Structure Refinement Details for $[N_2NH]Zr(CH_3)_2$ (1a), $[N_2NMe]Zr(CH_3)_2$ (1b), $\{[N_2NMe]Zr(CH_3)(Et_2O)\}[B(C_6F_5)_4]$ (2b), and $[\{[N_2NMe]Zr(CH_3)\}_2(\mu\text{-}CH_3)][B(C_6F_5)_4]$ (5b)[a]

	1a	1b	2b	5b
formula	$C_{34.0150}H_{49}N_3Zr$	$C_{25}H_{39}N_3Zr$	$C_{52}H_{46}BF_{20}N_3OZr$	$C_{73}H_{75}BF_{20}N_6Zr_2$
fw	596.99	472.81	1210.95	1609.66
cryst size (mm)	0.24 × 0.12 × 0.08	0.12 × 0.12 × 0.12	0.38 × 0.38 × 0.16	0.12 × 0.2 × 0.2
space group	$P2_1/c$	$Pnma$	$P2_1/n$	$P2_1/c$
a (Å)	18.740(11)	13.1319(8)	17.7775(3)	14.268(3)
b (Å)	10.874(5)	24.1909(14)	12.4765(2)	19.568(6)
c (Å)	17.541(7)	7.9669(5)	24.3498(5)	25.719(7)
α (deg)	90	90	90	90
β (deg)	110.54(4)	90	108.54(1)	93.46(3)
γ (deg)	90	90	90	90
V (Å^3)	3347(3)	2530.9(3)	5120.52(16)	7168(3)
Z	4	4	4	4
calcd density (g/cm^3)	1.185	1.241	1.571	1.492
μ (mm^{-1})	0.353	0.449	0.330	0.389
F(000)	1260	1000	2448	3268
T (K)	183(2)	192(2)	187(2)	183(2)
θ range (ω scans) (deg)	2.20−19.99	1.68−23.27	2.06−20.00	2.20−20.00
index ranges	$-20 \le h \le 18$	$-14 \le h \le 14$	$-16 \le h \le 17$	$-7 \le h \le 12$
	$-12 \le k \le 19$	$-26 \le k \le 16$	$-11 \le k \le 12$	$-14 \le k \le 18$
	$-14 \le l \le 19$	$-8 \le l \le 8$	$-20 \le l \le 23$	$-22 \le l \le 24$
no. of rflns collected	9623	9642	14 652	9897
no. of indep rflns	3122	1868	4753	6209
no. of data/restr/params	2977/0/353	1868/0/140	4753/0/704	6209/0/919
goodness of fit on F^2	1.118	1.113	1.343	0.907
R1/wR2 ($I > 2\sigma(I)$)	0.0692/0.1565	0.0526/0.1244	0.0663/0.1184	0.0532/0.0945
R1/wR2 (all data)	0.0945/0.1759	0.0788/0.1401	0.0736/0.1205	0.1350/0.1173
extinction coeff	0.0031(5)	0.0000(7)	0.00040(10)	0.0000(9)
max/min peaks (e/Å^3)	0.577/−0.354	0.432/−0.401	0.359/−0.340	0.461/−0.333

[a] All structures were solved on a Bruker CCD diffractometer using 0.710 73 Å Mo Kα radiation. [b] $R1 = \sum||F_o| - |F_c||/\sum|F_o|$. [c] $wR2 = [(\sum w(|F_o| - |F_c|)^2/\sum wF_o^2)]^{1/2}$.

Table 2. Bond Lengths (Å) and Angles (deg) for $[N_2NH]ZrMe_2$ (1a) and $[N_2NMe]ZrMe_2$ (1b)

	1a	1b
Zr−N(1)	2.095(6)	2.095(4)
Zr−N(2)	2.095(6)	2.095(4)
Zr−C(1)	2.248(9)	2.240(7)
Zr−C(2)	2.255(9)	2.265(7)
Zr−N(3)	2.387(7)	2.373(5)
N(1)−Zr−N(2)	140.0(3)	140.5(2)
N(1)−Zr−C(1)	102.1(3)	101.46(13)
N(1)−Zr−C(2)	102.3(3)	102.78(13)
N(1)−Zr−N(3)	70.1(2)	70.26(11)
N(2)−Zr−C(2)	103.4(3)	102.78(13)
N(2)−Zr−N(3)	70.3(2)	70.26(11)
N(2)−Zr−C(1)	101.8(3)	101.46(13)
C(1)−Zr−C(2)	102.3(3)	103.2(3)
C(1)−Zr−N(3)	135.1(3)	129.2(2)
C(2)−Zr−N(3)	122.6(3)	127.6(3)
Zr−N(1)−C(11)	121.8(5)	118.8(3)
Zr−N(2)−C(21)	120.4(5)	118.8(3)
N(1),Zr,N(3)/N(2),Zr,N(3)	174[a]	178[a]
C−N−C	116.5(7)	112.3(6)

[a] Obtained from a Chem 3D model.

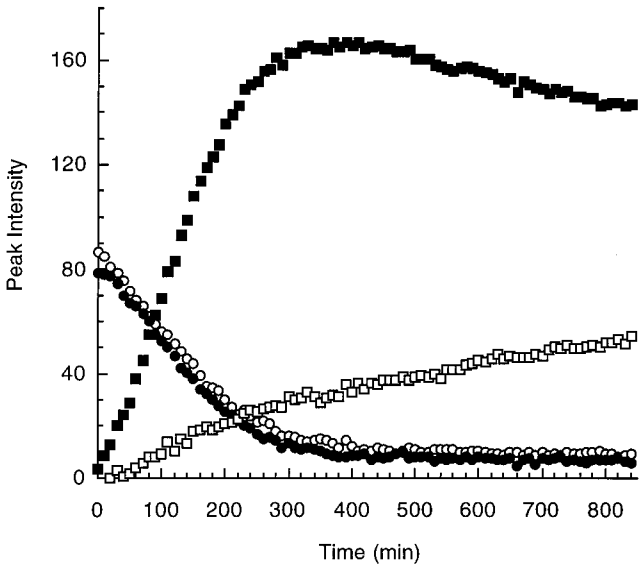

Figure 3. Peak intensities versus time for labeled methyl groups, as determined by ^{13}C NMR spectroscopy in C_6D_6, in a mixture of ***1a** ([$[N_2NH]Zr$*Me_2) and **1b** ($[N_2NMe]$-$ZrMe_2$): (●) ***1a**(eq); (○) ***1a**(ax); (■ ***1b**(eq); (□) ***1b**(ax). $[$***1a**$]_0 = 5.41$ mM; $[$**1b**$]_0 = 74.3$ mM. The intensities of ***1b** resonances have been corrected for the initial concentration of naturally abundant ^{13}C using the unlabeled N*Me* substituent as an internal standard.

ppm in the ^1H NMR spectrum and 37.10 ppm in the ^{13}C NMR spectrum.

Addition of $[N_2NMe]ZrMe_2$ (**1b**; 74.3 mM) to $[N_2NH]$-Zr*Me_2 (***1a**; 5.41 mM) led to a scrambling of the ^{13}C-labeled methyl groups in **1a** with the unlabeled groups (naturally abundant ^{13}C) in **1b** over a period of several hours. (The excess of **1b** ensures that >95% of the labeled methyl groups end up in **1b** and that labeled methyl groups disappear from ***1a** in a pseudo-first-order manner.) As shown in Figure 3, the labeled methyl groups in ***1a** scramble into **1b** completely in ∼7 h, but at that point the amount of labeled methyl group in the equatorial methyl position in ***1b** is 5.5 times the amount in the axial methyl position; i.e., a labeled methyl group scrambles from **1a** into **1b** specifically into an equatorial position, and axial/equatorial scrambling within partially and selectively labeled **1b** is relatively slow. (Assignment of the Zr−Me resonances is based upon 2D NMR studies, as described in the Experimental Section.) Note that *both* axial and equatorial labeled methyl groups disappear from ***1a** at approximately the same rate. The rate constant for the intermolecular methyl scrambling process from the data shown in

Scheme 2

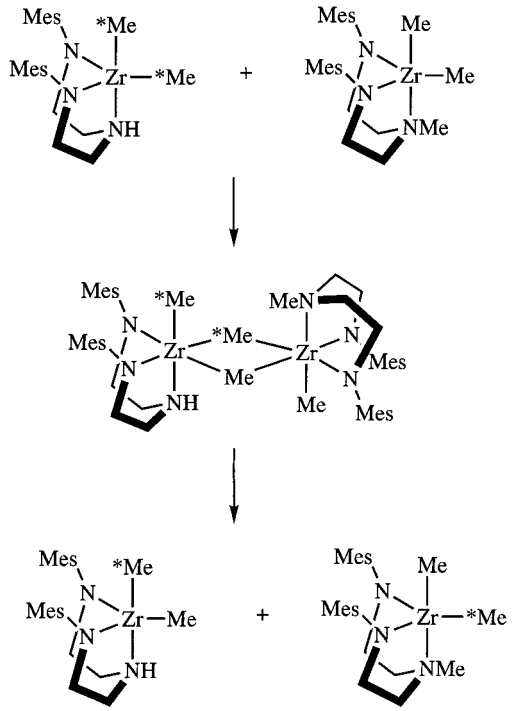

Figure 3 (60−330 min) is [8.2(4)] × 10^{-2} M^{-1} min^{-1}, while the first-order rate of axial/equatorial scrambling in **1b** (between t = 500 and 830 min) is [5.1(2)] × 10^{-4} min^{-1}. A plausible mechanism (Scheme 2) consists of formation of a dimeric species that contains a *fac* form of the ligand and equivalent bridging methyl groups *trans* to the amido ligands and pseudooctahedral coordination geometries around each Zr. This process would generate initially the [N_2NMe]Zr*Me$_{eq}$Me$_{ax}$ form of ***1b**. Intramolecular scrambling of *Me and Me within [N_2NMe]Zr*Me$_{eq}$Me$_{ax}$ to give [N_2NMe]ZrMe$_{eq}$*Me$_{ax}$ then could be accomplished via (for example) a pseudorotation process. Although it is not necessary to dissociate and invert the amine donor in order to scramble "axial" and "equatorial" methyl groups in a *fac* structure (or, alternatively, a methyl group *syn* with respect to the amine substituent with that *anti* with respect to the amine substituent in a *mer* structure), we cannot discount that possibility. However, we do not favor this option in view of the relatively electrophilic nature of zirconium. There is more than one possible reason axial and equatorial labeled methyl groups in **1a** both disappear at the same rate, the simplest being that axial/equatorial scrambling in **1a** is relatively fast, in contrast to **1b**. (As noted above, rapid axial/equatorial scrambling in **1a** could be responsible for the result shown in Scheme 1.) After considering a variety of potentially complicating mechanistic features of this scrambling process, and with the knowledge that alkyls scramble in other diamido/donor systems that we have been studying,[47,52] we have decided to revisit this process at a later date. One of the several interesting questions that at least should be stated in view of our focus in this paper on cationic (see below) and anionic (trimethyl) diamido/donor Zr complexes is whether methyl group exchange between Zr centers might be "ionic" rather than covalent: e.g., involve formation of a Zr^+Zr^- pair.

(52) Mehrkhodavandi, P. Unpublished observations.

Table 3. Selected Bond Lengths (Å) and Angles (deg) in {[N_2N(CH$_3$)]Zr(CH$_3$)(Et$_2$O)}[B(C$_6$F$_5$)$_4$]

Bond Lengths			
Zr(1)−C(1)	2.391(8)	Zr(1)−N(1)	2.014(7)
Zr(1)−O(1)	2.234(5)	Zr(1)−N(2)	2.426(6)
Zr(1)−N(3)	2.049(6)		

Bond Angles			
C(1)−Zr(1)−N(2)	87.3(2)	N(1)−Zr(1)−N(2)	70.1(2)
O(1)−Zr(1)−N(2)	170.5(2)	N(3)−Zr(1)−C(1)	114.0(2)
O(1)−Zr(1)−C(1)	90.7(2)	N(3)−Zr(1)−O(1)	99.9(2)
N(1)−Zr(1)−C(1)	109.5(3)	N(3)−Zr(1)−N(1)	119.9(3)
N(1)−Zr(1)−O(1)	119.3(2)	N(3)−Zr(1)−N(2)	72.5(2)
N(1),Zr,N(2)/ N(2),Zr,N(3)	132[a]	Zr(1)−N(1)−C(16)−C(21)	88.9(7)
		Zr(1)−N(3)−C(16)−C(17)	101.7(8)

[a] Obtained from a Chem 3D model.

Synthesis and Identification of Cations That Contain Diethyl Ether or Dimethylaniline. The reaction of **1a** or **1b** with 1 equiv of [Ph_3C][B(C$_6$F$_5$)$_4$] in chlorobenzene at −20 °C, followed by the addition of diethyl ether, led to compounds formulated as {[N_2NX]-Zr(CH$_3$)(ether)}[B(C$_6$F$_5$)$_4$] (X = H (**2a**), Me (**2b**); eq 2). These products were isolated as yellow powders in 80% (**2a**) and 90% (**2b**) yields upon addition of pentane.

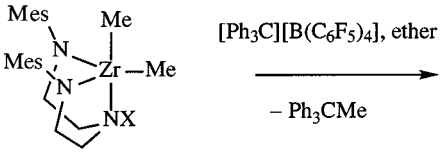

X = H (**1a**); Me (**1b**)

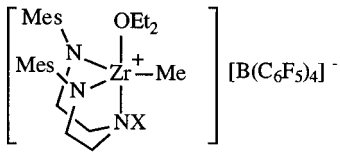

(2)

X = H (**2a**); Me (**2b**)

Single crystals of **2b** suitable for X-ray diffraction were grown from pentane/chlorobenzene at −28 °C (see Tables 1 and 3). Compound **2b**$^+$ (signifying the cation only) has a distorted-trigonal-bipyramidal structure in which the [N_2NMe]$^{2-}$ ligand is coordinated facially, the Zr−Me group (C(1)) is equatorial, and the diethyl ether is in an axial position (Figure 4), as shown by the N(1)−Zr−N(3) angle of 119.9(3)° and the O(1)−Zr−N(2) angle of 170.5(2)°. The sum of the angles at the oxygen is 358.0°, which indicates that it is close to being trigonal planar. Perhaps the most accurate measure of the nature of the ligand's coordination geometry is the angle between the N(1)−Zr−N(2) and N(3)−Zr−N(2) planes (132°), which is markedly reduced from what it is in **1a** (174°) and **1b** (178°) and is typical of a complex that has the "*fac*" structure, e.g., [(*t*-Bu-N-*o*-C$_6$H$_4$)$_2$O]ZrMe$_2$.[2] The Zr(1)−C(1) distance (2.391(8) Å) is approximately 0.1 Å *longer* than what it is in **1a** and **1b**. The N(3)−Zr(1)−N(1) angle (119.9(3)°) is the largest of the three N−Zr−N angles. The N_{amido}−Zr bond lengths (Zr(1)−N(1) = 2.014(7) Å, Zr(1)−N(3) = 2.049(6) Å) are similar to those in **1a** and **1b**, but the Zr(1)−N(2) distance (2.426(6) Å) is somewhat longer than a typical Zr−N_{donor} distance (∼2.30 Å). The structure of the [B(C$_6$F$_5$)$_4$]$^-$ anion is normal.

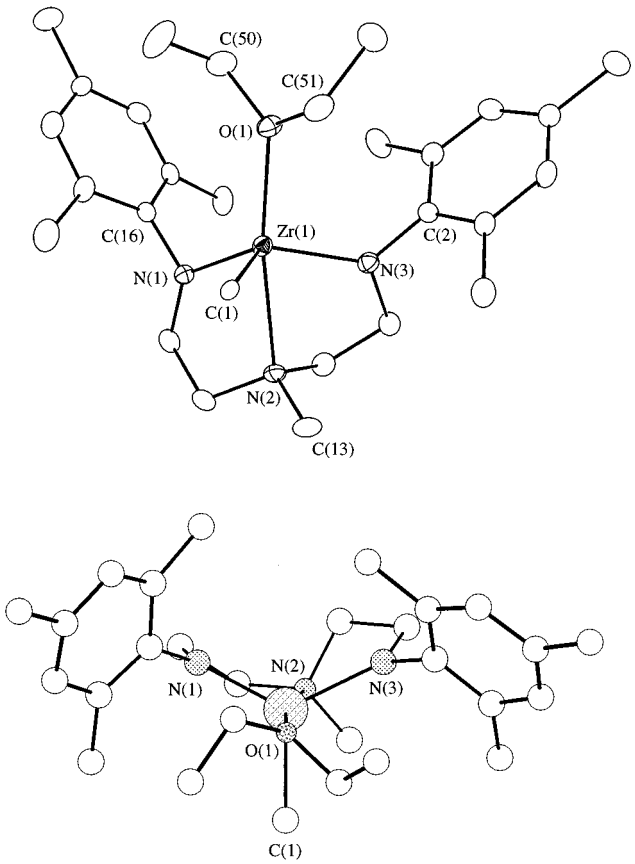

Figure 4. Views of $[N_2NMe]Zr(CH_3)(ether)\}^+$ (**2b**): (top) ORTEP diagram; (bottom) Chem 3D view down the O−Zr−N axis.

The VT NMR spectra (^1H and ^{13}C; −25 to 60 °C) of **2a** and **2b** in C_6D_5Br are consistent with the structure of **2b**$^+$ in the solid state. For example, the $^{13}C\{^1H\}$ NMR spectrum of **2b** (recorded for the $Zr(^{13}CH_3)$ complex) showed sharp resonances for the CH_3N (45.7 ppm) and CH_3Zr (39.8 ppm) groups (cf. 36.8 ppm for the NMe group and 42.5 and 39.9 ppm for the ZrMe groups in **1b**). In a 1:4 mixture of C_6D_5Br and $C_6D_5CD_3$ the Zr−CH_3 resonance is observed at 39.5 ppm at 22 °C and shifts to 38.5 ppm at −50 °C before the product crystallizes out of solution. The bound diethyl ether in **2b** does not exchange with free ether on the NMR time scale, as shown in spectra of samples to which ether has been added. The bound ether appears to freely rotate about the Zr−O bond on the NMR time scale, as evidenced by the overall mirror symmetry and equivalence of the four methylene protons. Rotation of the mesityl rings around the N−C_{ipso} bond is slow on the NMR time scale on the basis of the observation of inequivalent *o*-methyl groups and inequivalent aryl ring protons in a given mesityl group. A ^1H NMR NOEDIF experiment for complex **2b** at room temperature revealed a NOE (+1.4%) between the NCH_3 (2.38 ppm) and the $ZrCH_3$ (0.19 ppm) protons, consistent with the equatorial methyl ligand's proximity to the axial NCH_3 group. All other ^1H NMR resonances were assigned on the basis of similar NOE experiments. ^{19}F NMR spectra at −25 °C showed resonances for $[B(C_6F_5)_4]^-$ that are characteristic of an "uncoordinated" isotropic anion. Complexes **2a** and **2b** were stable in C_6D_5Br for several days at room temperature.

Addition of 1 equiv of $[PhNMe_2H][B(C_6F_5)_4]$ to a solution of **1b** in chlorobenzene yielded $\{[N_2NMe]Zr(CH_3)(NMe_2Ph)\}[B(C_6F_5)_4]$ (**3b**; eq 3) quantitatively. Compound **3b** could be isolated in 95% yield as a orange powder by addition of pentane to the chlorobenzene solution. NMR spectra of **3b** in C_6D_5Br between −10 and 60 °C are shown in Figure 5. All resonances were assigned on the basis of NOE experiments (e.g., see eq 4) and comparison with spectra of the analogous compound prepared from $[N_2N^*Me]Zr^{\#}Me_2$ (# implies 67% ^{13}C).

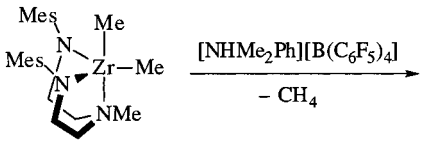

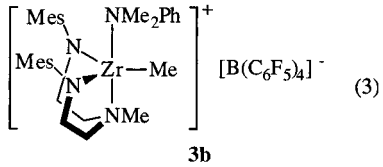

(3)

3b

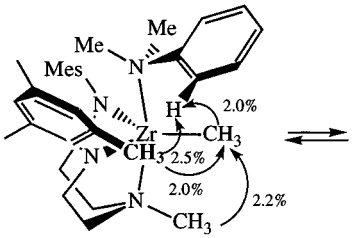

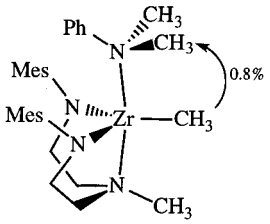

(4)

At 20 °C several resonances are broad, including that ascribed to $ZrCH_3$ at 0.07 ppm. At 60 °C all resonances are sharp and the spectrum is characteristic of a structure with C_s symmetry and nonrotating mesityl groups. At −10 °C only the resonance that can be ascribed to the mesityl *p*-methyl groups is sharp. ^1H NOEDIF experiments show that the dimethylaniline is bound in the apical pocket and is freely rotating about the Zr−N bond axis on the NMR time scale at 60 °C. In an analogous sample in which free NMe_2Ph had been added, resonances for the *ortho* aryl protons of both the coordinated dimethylaniline (5.67 ppm) and free dimethylaniline (6.80 ppm) were observed. This finding suggests that the rate of exchange between free and coordinated dimethylaniline is relatively slow ($<\sim 0.1$ s^{-1}) at 20 °C, while the rate of intramolecular motion responsible for the fluxional process that leads to broad resonances near room temperature must be on the order of $\sim 10^2$ s^{-1}. The $^{13}C\{^1H\}$ NMR spectrum at 20 °C of a sample prepared from $[N_2N^*Me]Zr^{\#}Me_2$ revealed a sharp resonance for the NCH_3 group (at 46.41 ppm) and a broad resonance for $ZrCH_3$ (at 37.0 ppm). The ^{19}F NMR spectrum of **3b** at 20 °C showed resonances characteristic of "free" $[B(C_6F_5)_4]^-$.

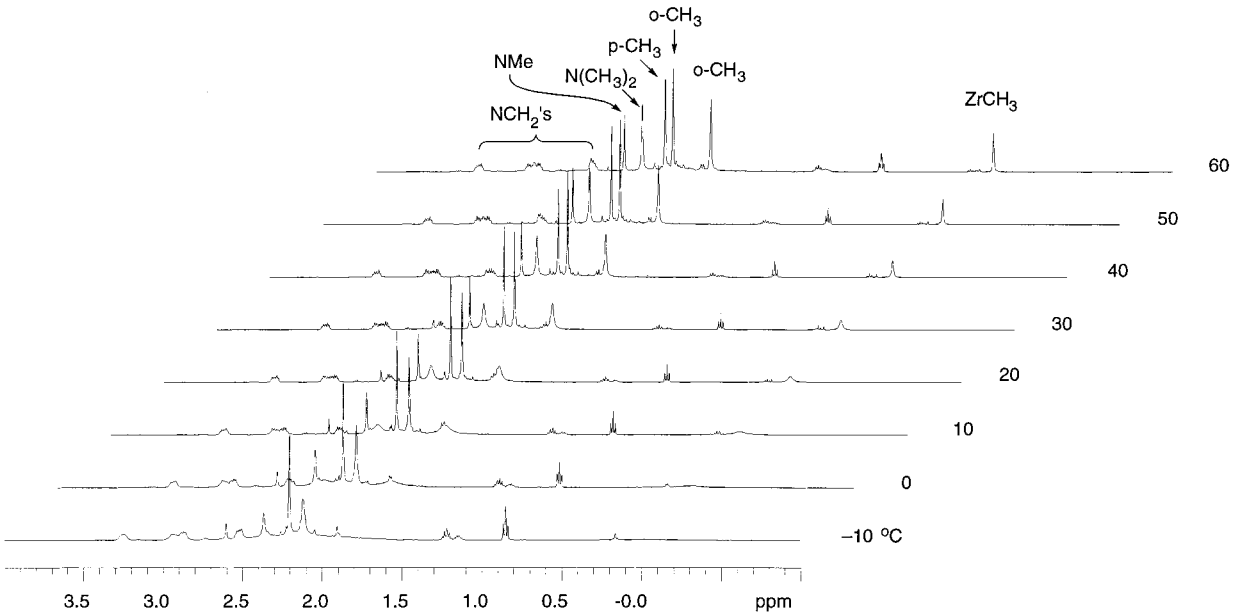

Figure 5. Variable-temperature ^{1}H NMR spectra (500 MHz, C_6D_5Br) of {[N_2N(CH$_3$)Zr](CH$_3$)(NMe$_2$Ph)}[B(C_6F_5)$_4$].

One possible explanation for broadening of most resonances at low temperatures is that the dimethylaniline adopts one of two different orientations within the coordination pocket due to a "cog-wheel" effect between it and the amido mesityl and axial amine methyl groups. The two possible orientations are shown in eq 4. The one in which the methyl group is located between the two mesityl rings would give rise to a molecule with no symmetry when rotation of the dimethylaniline in the pocket is slow. At 60 °C rapid rotation about the Zr−dimethylaniline bond would lead to a molecule with mirror symmetry on the NMR time scale. A variation of this explanation is that in the lowest energy species the ligand backbone is twisted with C(13) (Figure 4) lying on one side of the plane that contains C(13), Zr, and N(2), as found in the solid state. With such a backbone configuration the molecule would have no symmetry. In this case dimethylaniline could adopt either coordination mode, since the asymmetry would arise from the twist in the ligand backbone alone. Interconversion of "twisted" forms would also be part of the fluxional process that leads to overall mirror symmetry at higher temperatures. A preferred twist and a fluxional process based on interconversion of "twisted" forms have also been observed in related molecules that contain the [(*t*-Bu-N-*o*-C$_6$H$_4$)$_2$O]$^{2-}$ ion.[2] Finally, association of the anion at more than one point on any five-coordinate cation in principle could lead to different forms being observed at some low temperature, a type of phenomenon that we believe to be the case in pseudotetrahedral "{[N_2NMe]Zr(CH$_3$)}[B(C_6F_5)$_4$]" (see below). However, the anion is unlikely to associate nearly as strongly with a five-coordinate species as with a four-coordinate or weakly solvated species; therefore, we do not propose that this behavior is part of the temperature-dependent process shown in Figure 5.

Addition of diethyl ether to NMR samples of **3b** immediately yields **2b**, although addition of dimethylaniline to NMR samples of **2b** does not lead to the formation of any detectable **3b**, consistent with a preferred binding of diethyl ether to the cationic zirconium center. Since **3b**$^+$ is almost certainly sterically too crowded to react readily with another base in an associative manner, we suggest that dimethylaniline first dissociates from **3b**$^+$ to yield a "base free" cation and that diethyl ether then binds in place of dimethylaniline.

When **1b** was treated with a slight excess of [PhNMe$_2$H][B(C_6F_5)$_4$], the initial product was **3b**, according to NMR data. However, **3b** rapidly decomposed to yield methane and a new cationic zirconium complex that contained no ZrMe group. We propose that this new species is the product of C−H bond activation in the mesityl's *o*-methyl group (eq 5). The ^{1}H NMR spectrum

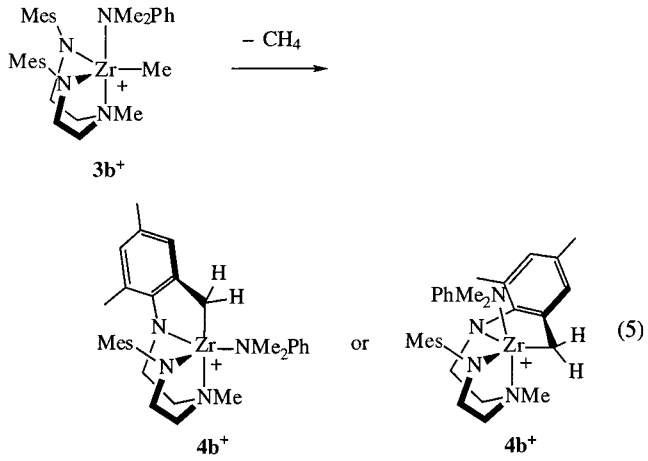

(5)

of **4b**$^+$ showed two doublets at 2.39 and 0.79 ppm (J_{HH} = 12.5 Hz) that can be assigned to the two inequivalent benzylic protons. Their coupling was confirmed in a ^{1}H gCOSY experiment. The remaining resonances have been assigned on the basis of ^{1}H ROESY and ^{1}H−^{13}C HMQC experiments (see the Experimental Section). We have observed and obtained structural confirmation that a "base-free" CH activated version is formed upon decomposition of {[N_2NMe]ZrMe}[B(C_6F_5)$_4$] (**6b**; see below)[47] and {[N_2NMe]Zr(CH$_2$CMe$_3$)}[B(C_6F_5)$_4$].[53] These results will be presented elsewhere. On the basis of this

(53) Schrodi, Y.; Bonitatebus, P. J., Jr. Unpublished observations.

structure, which is a dimeric dication with the activated mesityl rings behaving as η^6-arenes toward cationic Zr centers, an alternative possible structure for **4b**$^+$ contains dimethylaniline in the "apical" position and the benzylic methylene group in the "equatorial" position (eq 5). Compound **4b** has not yet been isolated in pure form. Only mixtures of **4b** and **3b** could be obtained by addition of pentane to a chlorobenzene solution.

Compound **4b** also could be obtained by decomposition of complex **3b** in chlorobenzene (4 h at 60 °C). The decomposition was monitored by ^{1}H NMR at 60 °C in C_6D_5Br to ~68% conversion (using a 21 mM sample). The reaction followed first-order kinetics with $k_{decomp} = [7.68(0.12)] \times 10^{-3}$ min^{-1}. Decomposition is clearly much more rapid in the presence of $[PhNMe_2H][B(C_6F_5)_4]$, as described above.

Reactions of [N$_2$NX]ZrMe$_2$ (X = H, CH$_3$) with 0.5 Equiv of Trityl. The reaction between $[N_2NMe]ZrMe_2$ and 0.5 equiv of $[Ph_3C][B(C_6F_5)_4]$ in chlorobenzene at −30 °C gave a pale yellow solution. NMR studies were consistent with the presence of a dimeric monocation, $[\{[N_2NMe]Zr(CH_3)\}_2(\mu\text{-}CH_3)][B(C_6F_5)_4]$ (**5b**; eq 6). Upon

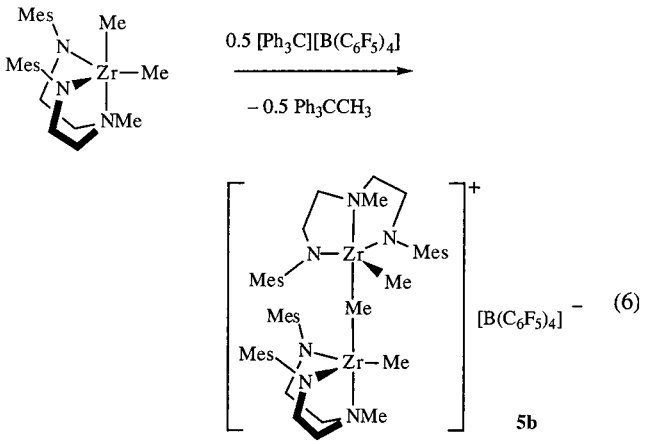

(6)

5b

addition of pentane, **5b** was isolated as a off-white powder in 87% yield. Unreacted $[N_2NMe]ZrMe_2$ was found when the reaction was carried out with less than 0.5 equiv of $[Ph_3C][B(C_6F_5)_4]$, while addition of 0.5−1.0 equiv of $[Ph_3C][B(C_6F_5)_4]$ to **1b** yielded mixtures of **5b** and $\{[N_2NMe]ZrMe\}[B(C_6F_5)_4]$ (**6b**) (see below).

Single crystals of **5b** suitable for X-ray diffraction were grown from a mixture of toluene and chlorobenzene at −28 °C. The solid-state structure of **5b**$^+$ can be described as an adduct of $\{[N_2NMe]ZrMe\}^+$ in which $[N_2NMe]ZrMe_2$ is the "base" that binds in an apical position (Figure 6; Tables 1 and 4). The bridging methyl group is approximately symmetrically bound between the two zirconium centers (2.508(9) and 2.457(9) Å), and a C_2 axis (not crystallographically imposed) that relates the two ends of the molecule passes through it. The $[B(C_6F_5)_4]^-$ anion is closer to one of the Zr centers than to the other in the crystal lattice. The Zr−C−Zr angle is close to linear (167.4(4)°). The hydrogen atoms on the central bridging methyl could not be located in the difference map. The Zr−C bond lengths to the terminal (equatorial) methyl groups (2.229(9) and 2.256(9) Å) are similar to the Zr−C bond lengths found in **1a**, **1b**, and **2b**$^+$. The two ends of **5b**$^+$ are staggered with respect to one another (~60°), as a consequence of the steric bulk and interlocking nature of the mesityl groups. The Zr−N

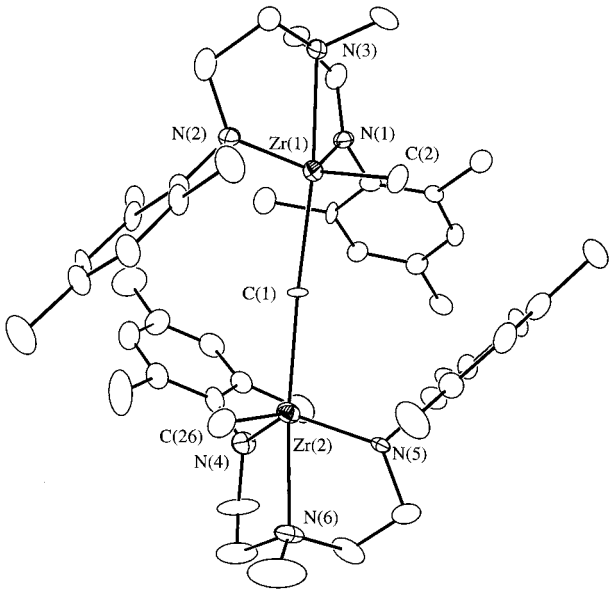

Figure 6. ORTEP drawing of the cation in complex **5b**.

Table 4. Selected Bond Lengths (Å) and Angles (deg) in [{[N$_2$N(CH$_3$)]Zr(CH$_3$)}$_2$[μ-(CH$_3$)]$^+$

Bond Lengths			
Zr(1)−C(1)	2.508(9)	Zr(2)−C(1)	2.457(9)
Zr(1)−C(2)	2.229(9)	Zr(2)−C(26)	2.256(9)
Zr(1)−N(1)	2.024(8)	Zr(2)−N(4)	2.049(8)
Zr(1)−N(2)	2.006(8)	Zr(2)−N(5)	2.015(8)
Zr(1)−N(3)	2.433(8)	Zr(2)−N(6)	2.455(8)

Bond Angles			
C(2)−Zr(1)−C(1)	97.2(3)	Zr(2)−C(1)−Zr(1)	167.4(4)
C(2)−Zr(1)−N(3)	92.4(4)	N(2)−Zr(1)−N(3)	71.9(3)
C(26)−Zr(2)−C(1)	94.8(3)	N(3)−Zr(1)−C(1)	170.1(3)
C(26)−Zr(2)−N(6)	85.4(4)	N(4)−Zr(2)−C(1)	113.2(4)
N(1)−Zr(1)−C(1)	102.7(3)	N(4)−Zr(2)−N(26)	112.3(4)
N(1)−Zr(1)−C(2)	113.1(3)	N(4)−Zr(2)−N(6)	71.6(4)
N(1)−Zr(1)−N(3)	71.0(3)	N(5)−Zr(2)−C(1)	103.9(3)
N(2)−Zr(1)−C(1)	107.2(3)	N(5)−Zr(2)−C(26)	109.3(3)
N(2)−Zr(1)−C(2)	108.3(3)	N(5)−Zr(2)−N(4)	120.2(4)
N(2)−Zr(1)−N(1)	124.5(3)	N(5)−Zr(2)−N(6)	70.9(3)
N(6)−Zr(2)−C(1)	174.5(4)		

bond lengths to the apical donor nitrogens (2.457(9) and 2.455(8) Å) are slightly longer (~0.04 Å) than in compound **2b**$^+$, while the Zr−N−C$_{ipso}$ angles are similar to those in **2b**$^+$ and **1b**.

NMR studies in C_6D_5Br suggest that **5b**$^+$ has a structure in solution that is similar to that found in the solid state. At −25 °C two sharp resonances are observed that correspond to the terminal (−0.38 ppm) and bridging (−0.89 ppm) ZrCH_3 groups, the former with twice the intensity of the latter. The average value of the $^1J_{CH}$ coupling constants in the bridging ZrCH_3 group is 133 Hz, which is consistent with C−H bonds that have a higher s character and which is significantly higher than for the terminal ZrCH_3 groups (115 Hz). As a consequence of the "interlocking" nature of the two ends of **5b**$^+$, more than four proton resonances are observed for the methylene protons in the two arms of the $[N_2NMe]^{2-}$ ligand and six inequivalent mesityl methyl groups are observed at −25 °C (Figure 7). The $^{13}C\{^1H\}$ NMR spectrum at −25 °C, recorded using ^{13}C-labeled **5b**$^+$, showed resonances for NCH_3 (45.02 ppm), terminal ZrCH_3 (41.23 ppm), and μ-CH_3 (40.11 ppm) groups as sharp singlets. These resonances were assigned on the basis of $^1H-^{13}C$ HMQC experiments.

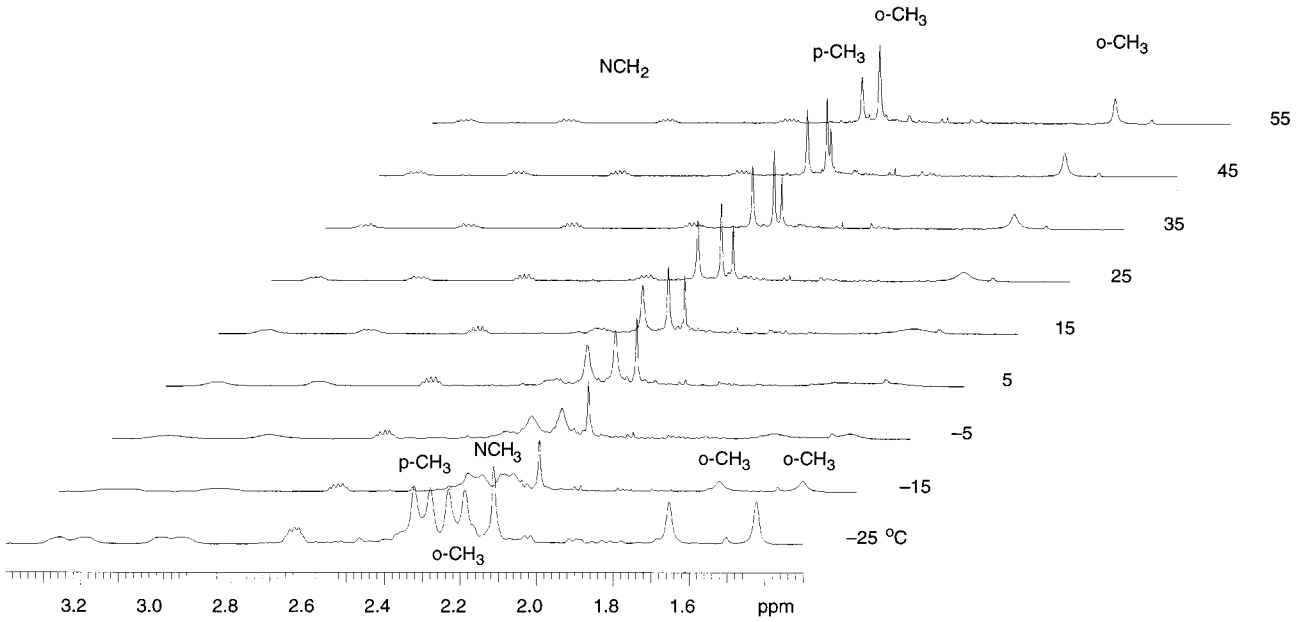

Figure 7. Variable-temperature ^{1}H NMR spectra (500 MHz, C_6D_5Br) of $[\{[N_2N(CH_3)Zr](CH_3)\}_2(\mu\text{-}CH_3)][B(C_6F_5)_4]$.

^{1}H ROESY experiments at −25 °C were consistent with the configuration at each metal in the solid state. The most relevant NOE (negative) cross-peak was the one between the terminal ZrCH_3 and the NCH_3 resonances. No cross-peaks were found between the bridging ZrCH_3 and the NCH_3 resonances. This result is consistent with the fact that the terminal $ZrCH_3$ groups occupy equatorial positions and the bridge is formed by a shared apical $ZrCH_3$ group. NOE cross-peaks were observed between one set of *o*-CH_3 groups of the mesityl substituents and the terminal ZrCH_3 group. NOE cross-peaks also were observed between the other set of *o*-CH_3 groups (the "inside" set at one metal center) with the bridging ZrCH_3 resonance. The ^{1}H ROESY experiment at −25 °C also showed EXSY (positive) cross-peaks between resonances for inequivalent mesityl groups. This was especially clear in the case of one *o*-CH_3 group (at ∼1.6 ppm) and indicates that the two inequivalent mesityl groups are exchanging.

A variable-temperature ^{1}H NMR study (Figure 7) revealed that at 55 °C each metal has mirror symmetry on the NMR time scale. This process cannot consist of reversible loss of $[N_2NMe]ZrMe_2$ from **5b**$^+$, since separate resonances for $[N_2NMe]ZrMe_2$ and **5b**$^+$ are observed at 50 °C in a sample of **5b**$^+$ to which $[N_2NMe]ZrMe_2$ has been added. The resonance for one *ortho* mesityl methyl set (at ∼1.55 ppm) is somewhat broader than the other at this temperature, but it is clear that rotation about the Mes−N bonds is still slow on the NMR time scale. The fluxional process does not affect the $ZrCH_3$ and NCH_3 resonances, which are sharp singlets in both ^{1}H and ^{13}C{^{1}H} NMR spectra between −25 and 65 °C. (The NCH_3 and *o*-CH_3 resonances are coincident at 55 °C in Figure 7.) The rate of this fluxional process was measured by line shape analysis of the two *o*-CH_3 resonances near 1.5 and 1.6 ppm between 248 and 330 K. An Eyring plot yielded $\Delta H^{\ddagger} = 12.5(3)$ kcal mol^{-1} and $\Delta S^{\ddagger} = -3.4(1.2)$ cal mol^{-1} K^{-1}. A process that consists of pure rotation of the two ends of the dimer with respect to one another seems improbable on steric grounds, as the mesityl rings would appear to be unable to pass one another readily. Therefore, we propose a process in which the two terminal methyl groups are pushed into bridging positions as the molecule "folds up" using the bridging methyl group as a "hinge" (eq 7). The transi-

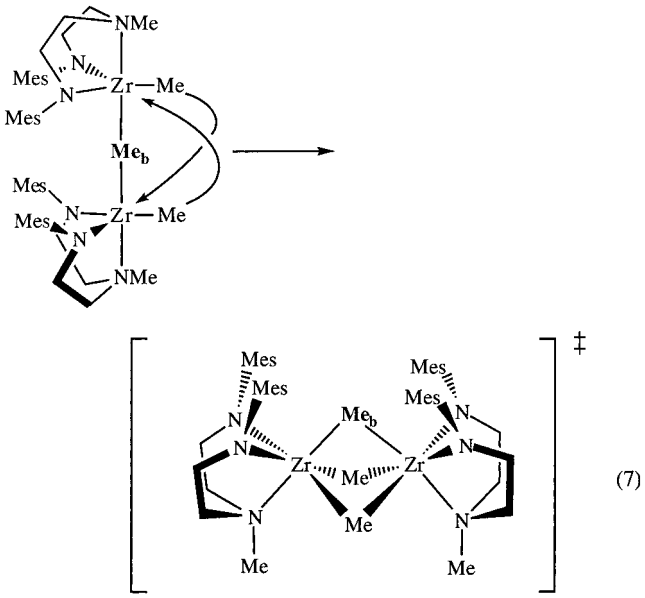

(7)

tion-state structure is then a dinuclear species that has three bent methyl bridges between two six-coordinate Zr atoms (two face-sharing pseudooctahedra), in which a mirror plane passes through Me_b and the NMe groups. Note that the bridging methyl group does *not* exchange with a terminal methyl group in this proposed mechanism, which is consistent with what is observed experimentally. The pseudooctahedral structure about each Zr in the dimeric species shown in eq 7 is reminiscent of pseudooctahedral *fac* species proposed in other methyl exchange reactions (Schemes 1 and 2).

In a ^{1}H ROESY experiment at 45 °C, EXSY (positive) cross-peaks were observed between the resonances for the terminal and bridging methyl groups and between the resonances for the two inequivalent *o*-CH_3 groups

in the mesityl groups, which suggests that terminal and bridging methyl groups are exchanging on the chemical time scale at this temperature, as are the two mesityl *o*-methyl groups. Bridging and terminal methyl groups exchange at rates on the order of $\sim 10^{-1}$ s^{-1} (at 45 °C), whereas at 45 °C the rate of intermetallic exchange of terminal methyl groups is approximately 4000 s^{-1}. At 25 °C the ROESY spectrum shows no EXSY (positive) cross-peaks that would signal exchange of terminal and bridging methyl groups.

Since **5b**$^+$ is essentially a $[N_2NMe]ZrMe_2$ adduct of "$\{[N_2NMe]ZrMe\}^+$", we might suspect that $[N_2NMe]ZrMe_2$ is lost readily from $[\{[N_2NMe]ZrMe\}_2(\mu\text{-}Me)]^+$ on the chemical time scale. This was confirmed by observing ^1H and $^{13}C\{^1H\}$ NMR spectra of a mixture of $[N_2NMe]Zr{*}Me_2$ and **5b** (1:2 ratio) in C_6D_5Br at 22 °C 10 min after mixing. By this time the Zr−methyl groups in $[N_2NMe]Zr{*}Me_2$ had scrambled with the unlabeled Zr−methyl groups in **5b** to produce a mixture in which *Me was present statistically in all Zr−methyl positions in all species. Therefore, the process shown in eq 8 must

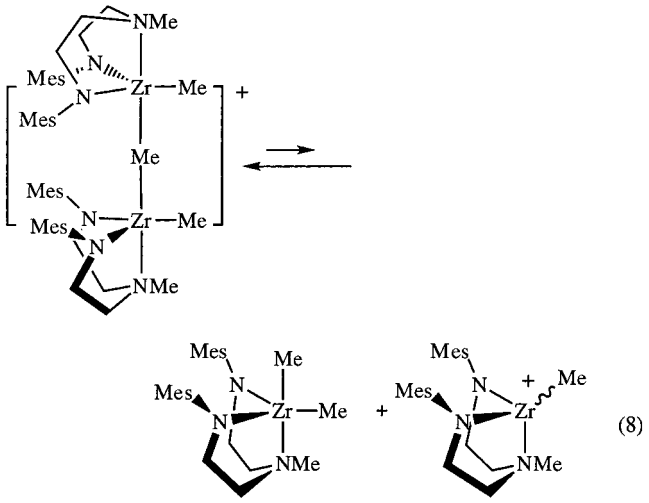

(8)

be rapid at 22 °C relative to the rate of exchange of equatorial and axial methyl groups in $[N_2N{*}Me]Zr{*}Me_2$ and bridging and terminal methyl groups in **5b**. The fact that **5b** is readily isolated suggests that the equilibrium constant for the dissociation shown in eq 8 probably is relatively small. We know that **5b** reacts with 1 equiv of trityl readily to give "$\{[N_2NMe]ZrMe\}^+$" (see below) but do not know whether it does so in a direct way or as a result of the dissociation shown in eq 8: i.e., via $[N_2NMe]ZrMe_2$.

Compound **5b** is surprisingly stable in C_6D_5Br solution. Some decomposition was observed after 5 min at 65 °C or after 1 day at 20 °C. Formation of methane could be confirmed, but the decomposition product or products could not be identified. Addition of 0.5 equiv of $[Ph_3C][B(C_6F_5)_4]$ to **1a** in C_6D_5Br yielded a species analogous to **5b**, namely $[\{[N_2NH]Zr(CH_3)\}_2(\mu\text{-}CH_3)][B(C_6F_5)_4]$ (**5a**), according to NMR spectra. Two zirconium methyl resonances are found in both ^1H and ^{13}C NMR spectra in a 2:1 ratio. A ^1H ROESY experiment at −10 °C showed negative (NOE) cross-peaks for the terminal and bridging methyl groups; i.e., the two are not exchanging readily at this temperature. All NMR data suggest that the structure of **5a** is similar to that of **5b**.

Addition of 1 equiv of $[Ph_3C][B(C_6F_5)_4]$ to ^{13}C-labeled **1a** in C_6D_5Br followed by addition of 1 equiv of **1b** yielded a statistical mixture of **5a**, **5b**, and $[\{[N_2NMe]Zr(CH_3)\}(\mu\text{-}CH_3)\{[N_2NH]Zr(CH_3)\}][B(C_6F_5)_4]$ in which the ^{13}C label was scrambled throughout the ZrMe positions. These data suggest that intra- and intermolecular scrambling processes discussed above for **1b** and **5b** are also found in **1a** and **5a**. For example, formation of $[\{[N_2NMe]Zr(CH_3)\}(\mu\text{-}CH_3)\{[N_2NH]Zr(CH_3)\}][B(C_6F_5)_4]$, in which the ^{13}C label is completely scrambled between the bridging and terminal positions, suggests that dissociation of any neutral dimethylzirconium complex from "$\{[N_2NX]Zr(CH_3)\}^+$" (X = H, Me) is fast on the chemical time scale (seconds).

Reactions of $[N_2NX]Zr(CH_3)_2$ (X = H, CH_3) with 1 Equiv or More of $[Ph_3C][B(C_6F_5)_4]$. The reaction between $[N_2NMe]Zr(CH_3)_2$ and 1 equiv of $[Ph_3C][B(C_6F_5)_4]$ in C_6D_5Br at −30 °C produces a yellow solution. The ^1H NMR spectrum of this solution at 20 °C revealed that Ph_3CCH_3 had formed quantitatively, along with a species having a methyl resonance at 0.15 ppm, consistent with formation of $\{[N_2NMe]Zr(CH_3)\}[B(C_6F_5)_4]$ (**6b**). As a sample of **6b** is cooled to −35 °C, the methyl resonance broadens and a resonance begins to grow in near −0.02 ppm and to increase in intensity; the resonances for what we shall call **6b$_1$** (near 0.15 ppm) and **6b$_2$** (near −0.02 ppm) sharpen at lower temperatures (Figure 8a). The ratio of the two resonances at −35 °C is close to 1:1. This behavior is repeatable and reversible. (For the moment we will ignore the small peak at −0.15 ppm, although it also appears to be a part of this temperature-dependent process.) The proportion of **6b$_2$** in the **6b$_1$**/**6b$_2$** mixture decreases as the temperature is increased (Figure 8a), and **6b$_1$** begins to interconvert with **6b$_2$**. The equilibrium constant, $K_{eq} = [\mathbf{6b_1}]/[\mathbf{6b_2}]$, was measured between 254 and 273 K at a concentration of 22 mM. Values of $\Delta H° = 7.9(5)$ kcal mol^{-1} and $\Delta S° = 32(3)$ cal mol^{-1} K^{-1} were obtained from a van't Hoff plot. Upon dilution of the sample (from [Zr] = 53 to 26 mM), isomer **6b$_2$** was the dominant species at low temperatures. Interconversion of **6b$_1$** and **6b$_2$** between −35 and 20 °C was modeled by line shape analysis (Figure 8b), taking into account the observed change in the amount of **6b$_1$** and **6b$_2$** at various temperatures, as calculated from the temperature dependence of *K* close to and above the coalescence point. An Eyring plot (248−293 K) led to values of $\Delta H^‡ = 16.3(5)$ kcal mol^{-1} and $\Delta S^‡ = 8(2)$ cal mol^{-1} K^{-1} for the conversion of **6b$_2$** to **6b$_1$**.

The two new species, **6b$_1$** and **6b$_2$**, have mirror symmetry on the NMR time scale and appear be two isomers of "$\{[N_2NMe]Zr(CH_3)\}[B(C_6F_5)_4]$". The ^{19}F NMR spectrum of the mixture at −25 °C showed resonances consistent with "uncoordinated" $[B(C_6F_5)_4]^-$ at chemical shifts that are virtually identical with those found in other ionic compounds reported here. Complex **6b** was stable in C_6D_5Br solution at −25 °C for days, but it decomposed at room temperature after 60 min, producing methane at the expense of the $ZrCH_3$ group. Preliminary results[47] to be reported in full elsewhere confirm that this product is a solvent-free dimer of **4b**$^+$.

The reaction between $[N_2N(*CH_3)]Zr(^{\#}CH_3)_2$ and $[Ph_3C][B(C_6F_5)_4]$ yielded the same isotopic distribution of ^{12}C and ^{13}C in the NMe and ZrMe groups in **6b$_1$** and **6b$_2$**

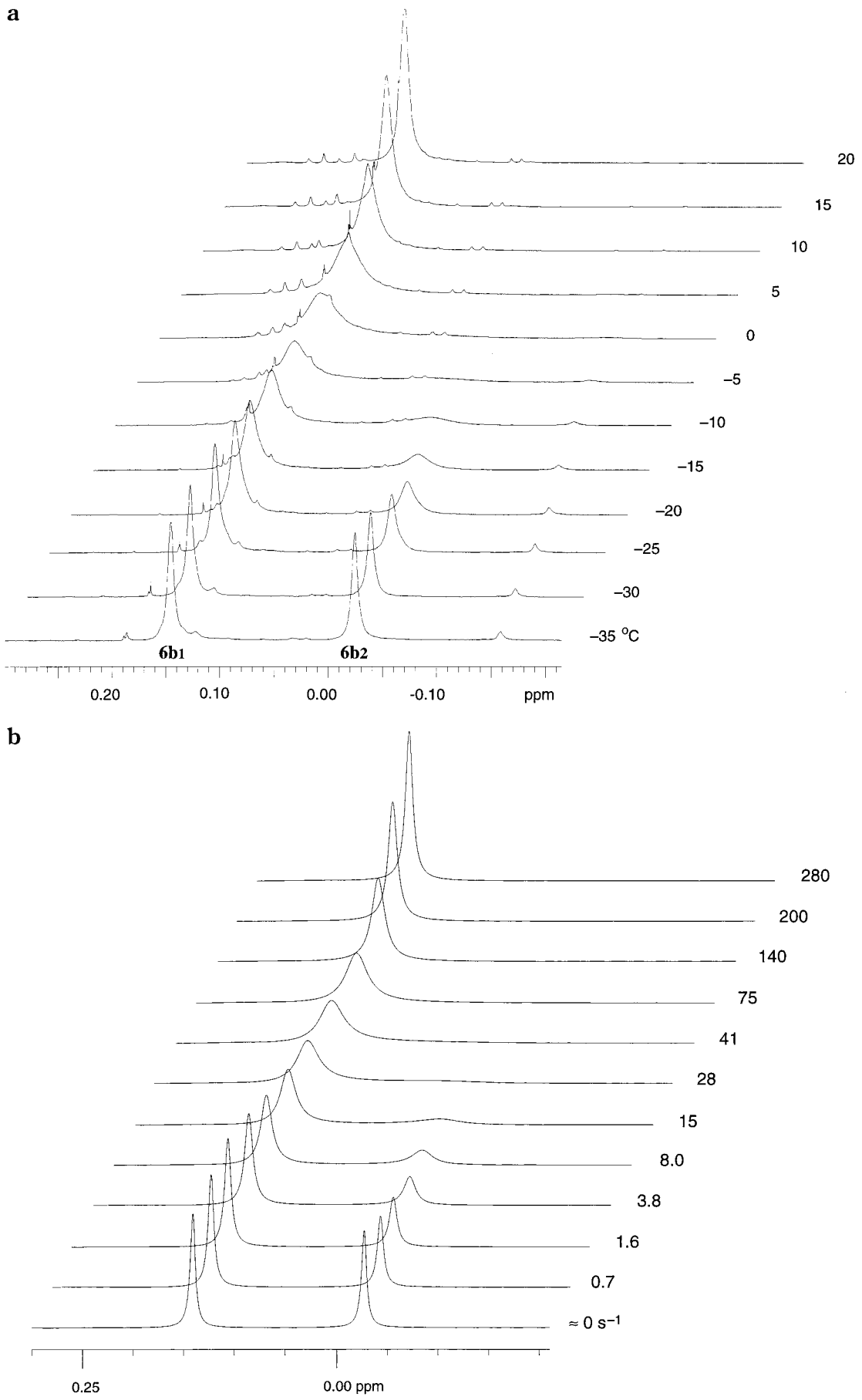

Figure 8. (a, top) Variable-temperature ^{1}H NMR spectra (500 MHz, C_6D_5Br) of the ZrCH_3 resonances in a mixture of **6b**$_1$ and **6b**$_2$. (b, bottom) Computer simulation and first-order rate constants ($k_{1,2}$) in s^{-1}.

(and triphenylethane) as in $[N_2N(*CH_3)]Zr(^{\#}CH_3)_2$; i.e., the products appeared to be "$\{[N_2N(*CH_3)]Zr(^{\#}CH_3)\}^+$" and $Ph_3C^{\#}CH_3$ (# implies 67% ^{13}C; * implies 100% ^{13}C). The $^{13}C\{^1H\}$ NMR spectrum of "$\{[N_2N(*CH_3)]Zr(^{\#}CH_3)\}^+$" at −25 °C showed sharp resonances for the NCH_3 groups at 45.47 ppm in **6b$_1$** and 46.51 ppm in **6b$_2$**. Both resonances are downfield of where they are observed in $[N_2N(*CH_3)]Zr(^{\#}CH_3)_2$ (35.9 ppm). In **6b$_1$**, the Zr−Me resonance is found at 47.25 ppm, downfield with respect to those in $[N_2N(*CH_3)]Zr(^{\#}CH_3)_2$ (40.7 and 42.7 ppm), similar to the chemical shift for an equatorial methyl group in **2b** and **3b**. However, the Zr−Me resonance in **6b$_2$** appeared at 33.52 ppm, which is a significantly higher field position than found for the ZrMe group in **6b$_1$**.

Similar behavior is observed for the $ZrCH_3$ resonance by both proton and carbon NMR in a 1:4 mixture of C_6D_5Br and $C_6D_5CD_3$. For example, a 10 mM sample showed resonances only for **6b$_2$** down to −20 °C, where the $ZrCH_3$ carbon resonance was observed at 32.67 ppm and the proton resonance at −0.078 ppm. At −30 °C two carbon resonances were observed at 32.49 and 32.33 ppm and two proton resonances at −0.135 and −0.187 ppm. Below −50 °C these resonances broadened and decreased in intensity as an oil precipitated from solution. The precise nature of the two forms of **6b$_2$** below −30 °C *in this mixed solvent* is not known.

On the basis of ^1H ROESY experiments at −35 °C, the structures of **6b$_1$**$^+$ and **6b$_2$**$^+$ in solution appear to be similar to the structures of **2b**$^+$, **3b**$^+$, and **5b**$^+$. The ^1H ROESY spectrum of "$\{[N_2N(*CH_3)]Zr(^{\#}CH_3)\}^+$" shows intense EXSY (positive) cross-peaks between related signals of both complexes, which confirms that **6b$_1$**$^+$ and **6b$_2$**$^+$ are in equilibrium. As we shall elaborate upon in the Discussion, all evidence points toward **6b$_1$**$^+$ and **6b$_2$**$^+$ being two types of $\{[N_2NMe]Zr(CH_3)\}[B(C_6F_5)_4]$ ion pairs.

The reaction of $[N_2NH]Zr(CH_3)_2$ with $[Ph_3C][B(C_6F_5)_4]$ in C_6D_5Br also led to a yellow solution. In this case, along with the signal corresponding to Ph_3CCH_3, the ^1H NMR spectrum at −25 °C suggested the quantitative formation of only one major new complex analogous to **6b$_2$**: i.e., **6a$_2$** (eq 9). Assignment was made on the basis

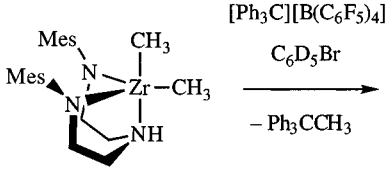

$\{[N_2NH]ZrMe\}[B(C_6F_5)_4]$ (**6a$_2$** only) (9)

of the chemical shift of the $ZrCH_3$ resonance at −0.13 ppm in the ^1H NMR spectrum and at 31.3 ppm in the $^{13}C\{^1H\}$ spectrum (recorded using the ^{13}C-labeled complex). (We must assume that chemical shifts in the two species are a reliable indicator of their nature.) At 20 °C only one broad resonance for the Zr−Me group was observed in both the ^1H (−0.08 ppm) and $^{13}C\{^1H\}$ (31.70 ppm) NMR spectra. An ^1H ROESY experiment at −25 °C showed a NOE (negative) cross-peak between signals of the $ZrCH_3$ and N*H* (2.88 ppm) groups and between one *o*-CH_3 group in the mesityl substituents with the $ZrCH_3$ group. According to these studies, the basic structure of **6a$_2$**$^+$ is similar to that of **6b$_1$**$^+$ and **6b$_2$**$^+$ and other monomeric ionic species discussed here (**2b**$^+$ and **3b**$^+$).

A solution that contains a mixture of complexes **6a** and **6b** was investigated via a ^1H ROESY experiment at −25 °C. For this purpose, a sample was prepared by mixing two freshly prepared solutions (∼53 mM) of each in C_6D_5Br. A chemical interconversion of **6b$_1$** and **6b$_2$** was indicated (EXSY cross-peaks for the ZrMe groups), but *not* between **6a$_2$** and **6b$_1$** or **6a$_2$** and **6b$_2$**. Another experiment was carried out in which Zr(*Me)-labeled **6a** was mixed with unlabeled **6b**; no incorporation of the ^{13}C label into **6b** was observed. Both experiments suggest that ZrMe groups *do not exchange* between **6a** and **6b** readily on the chemical time scale.

Discussion

The *mer* structures for **1a** and **1b** that were found in the solid state (versus *fac* structures) were initially surprising to us. However, the flexibility of the arms that connect the amine nitrogen with the amido nitrogens apparently allows the tetrahedral amine donor to be accommodated in a *mer* structure. Orientation of the plane of the aryl rings perpendicular to the plane of the amido nitrogen is favored for steric reasons and was noted initially by McConville in a variety of titanium and zirconium complexes.[14−16,18−21,23,24] There is little steric hindrance between the aryl groups and the equatorial methyl ligands. Therefore, the structure has essentially no tendency to "twist" into a *fac* form. Steric interaction between the *tert*-butyl groups and the methyl groups in a *mer* structure is thought to be one of the main reasons why $[(t\text{-Bu-N-}o\text{-}C_6H_4)_2O]ZrMe_2$ has a *fac* structure in the solid state, while $[(i\text{-Pr-N-}o\text{-}C_6H_4)_2O]ZrMe_2$ has a *mer* structure.[2,12] In contrast, the core structures of the two "base adducts" (**2b**$^+$ and **5b**$^+$) are *fac* with the base (diethyl ether or $[N_2NMe]$-$ZrMe_2$, respectively) bound in an apical position *trans* to the amine donor. This is the same type of structure that is observed for $\{[(t\text{-Bu-N-}o\text{-}C_6H_4)_2O]ZrMe\}[MeB(C_6F_5)_3]$, in which the "base" is $[MeB(C_6F_5)_3]^-$.[2,3] One might have predicted in each system that the equatorial site would have been the least hindered position sterically and that the base would bind there. However, the top view of **2b** shown in Figure 4 emphasizes that the "outside" *o*-methyl groups on each mesityl ring might interact sterically to a significant degree with whatever ligand is in the equatorial position and that a methyl group might be the least demanding sterically in the equatorial position compared to diethyl ether or $[N_2NMe]ZrMe_2$. It should be noted that the six-coordinate structure of $\{[(t\text{-Bu-N-}o\text{-}C_6H_4)_2O]ZrMe(\text{dimethoxyethane})\}^+$ is essentially *fac*, with the *methyl* group in the apical position and one of the dme oxygens binding weakly to an upper CON face,[2] and that pseudooctahedral $\{[(t\text{-Bu-N-}o\text{-}C_6H_4)_2O]ZrMe(THF)_2\}^+$ contains the ligand in the *mer* configuration with the two THF ligands *trans* to one another.[2]

There is much precedent for the formation of *neutral* homometallic M(*μ*-Me)M species in the literature, where M is a transition metal, lanthanide, or actinide: e.g., Zr(*μ*-Me)Zr,[54−57] Lu(*μ*-Me)Lu,[58] and U(*μ*-Me)U species.[59]

(54) Buchwald, S. L.; Lucas, E. A.; Davis, W. M. *J. Am. Chem. Soc.* **1989**, *111*, 397.

However, more relevant to the formation of **5a**$^+$ and **5b**$^+$ are *monocationic* species that contain a bridging methyl group: e.g., various [Zr(μ-Me)Zr]$^+$ species[60−64] and a [Th(μ-Me)Th]$^+$species.[65] In all cases the compounds are derived from metallocenes. Metallocenes and metallocene cations have received intense scrutiny in the last 15 years, in particular with respect to cations as relatively well-defined catalysts for the polymerization of ethylene and terminal olefins. We believe **5b**$^+$ to be the first example of a "non-metallocene" monocationic [M(μ-Me)M]$^+$ species. Its formation is sensible on the basis of published metallocene [Zr(μ-Me)Zr]$^+$ structures, the ability of methyl groups to bridge in a linear or bent manner between two of the same or two different metals (including main-group metals), and the formation of other cationic species described here that contain a "base" less exotic than [N$_2$NMe]ZrMe$_2$, e.g., diethyl ether or dimethylaniline. Although we could not locate the protons on the bridging methyl group in **5b**$^+$, the approximately equal Zr−(μ-Me) bond lengths, along with the large CH coupling constant, suggest that the methyl group is essentially planar, as found in several other neutral and monocationic Zr−(μ-Me)Zr species.

One of the most important questions that we must address here is the nature of **6b$_1$** and **6b$_2$**. We have considered several explanations and have decided on the basis of results in the literature, in particular relatively recent studies by Marks[66] and calculations by Ziegler,[67] that only one explanation can be argued successfully: namely, that **6b$_1$** and **6b$_2$** are different ion pairs whose interconversion at low temperatures is slow enough to observe on the NMR time scale. (There are three different faces in an untwisted tetrahedral cation such as **6b**$^+$; therefore, three possible ion pairs could be observed in theory, two of which have mirror symmetry.) Before we discuss the nature of the ion pairs, we should outline some of the findings of Marks and Ziegler for metallocene and constrained-geometry catalysts.

There is now a significant amount of evidence that [MeB(C$_6$F$_5$)$_3$]$^-$ can associate relatively strongly with a pseudo-three-coordinate metallocene cation. Marks and his group in particular have experimentally measured both the rate of migration of the B(C$_6$F$_5$)$_3$ fragment from one methyl group to the other in a neutral metallocene dimethyl complex and the rate of migration of the [MeB(C$_6$F$_5$)$_3$]$^-$ ion from one position in the pseudotetrahedral ion pair to the other.[66,68] In {(η^5-1,2-Me$_2$C$_5$H$_3$)$_2$ZrMe}[MeB(C$_6$F$_5$)$_3$] in toluene at 298 K the rate of migration of the B(C$_6$F$_5$)$_3$ fragment was found to be 3×10^{-3} s^{-1}, while the rate of migration of the [MeB(C$_6$F$_5$)$_3$]$^-$ ion was found to be 30×10^{-3} s^{-1}. In chlorobenzene the rates were found to be 60 and 2.0×10^4 s^{-1}, respectively. Unfortunately, analogous systems in which the anion is [B(C$_6$F$_5$)$_4$]$^-$ are unstable. Therefore, it was not possible to measure the rate of [B(C$_6$F$_5$)$_4$]$^-$ ion migration and compare it to the rate of [MeB(C$_6$F$_5$)$_3$]$^-$ ion migration.

A recent paper by Ziegler explores these issues and others theoretically using DFT calculations for (η^5-1,2-Me$_2$C$_5$H$_3$)$_2$ZrMe$_2$ combined with various Lewis acids, including {(η^5-1,2-Me$_2$C$_5$H$_3$)$_2$ZrMe}[B(C$_6$F$_5$)$_4$] species.[67] His calculations reproduce the experimental findings of Marks for species that contain the [MeB(C$_6$F$_5$)$_3$]$^-$ ion.[66,68] Moreover, Ziegler calculates that, upon changing the solvent from toluene to chlorobenzene, the ion pair dissociation energy (ΔH_{ips}) for the [MeB(C$_6$F$_5$)$_3$]$^-$ ion decreases from 38.0 to 23.4 kcal mol^{-1}, or about 40%, while upon changing to the [B(C$_6$F$_5$)$_4$]$^-$ ion in toluene, ΔH_{ips} drops to 22.0 kcal mol^{-1}. No value for ΔH_{ips} for the [B(C$_6$F$_5$)$_4$]$^-$ ion in chlorobenzene was provided, but if ΔH_{ips} were to drop from 22.0 kcal mol^{-1} by 40%, we would expect ΔH_{ips} for the [B(C$_6$F$_5$)$_4$]$^-$ ion in chlorobenzene to be ∼13 kcal mol^{-1}. Ziegler notes that no zirconium cation/anion pairs are ever likely to be "completely solvated." Nevertheless, calculated ΔH_{ips} values are a good measure of the degree of cation/anion interaction in various solvents and, in particular, the degree to which the anion might bind in a given position on a pseudotetrahedral cation. All ΔH_{ips} values will depend dramatically on the steric crowding in the cation, the degree to which the negative charge is delocalized in the anion, the nature of the anion, etc.

To our knowledge there are no experimental results in the literature which suggest that different ion pairs in which [B(C$_6$F$_5$)$_4$]$^-$ is the anion can be observed at low temperatures. It should be noted, however, that an X-ray structure of {Cp*$_2$ThMe}[B(C$_6$F$_5$)$_4$] shows [B(C$_6$F$_5$)$_4$]$^-$ to be associated with the Th through F$_{ortho}$ and F$_{meta}$ interactions in one ring, with the Th−F distances being longer than the relevant Th^{4+} and F$^-$ ionic radii.[65] Interestingly, however, the ^{19}F NMR spectrum in toluene-d_8, a solvent in which the anion might be expected to be more *strongly* associated with the cation than in chlorobenzene, showed magnetically equivalent C$_6$F$_5$ rings down to −70 °C. This result suggests that although the association of the {Cp*$_2$ThMe}$^+$ cation and the [B(C$_6$F$_5$)$_4$]$^-$ anion is strong enough to isolate a crystalline adduct, the [B(C$_6$F$_5$)$_4$]$^-$ anion must be "tumbling" rapidly on the NMR time scale (>100 s^{-1}) between various types of Th−F interactions and from one C$_6$F$_5$ ring to the other, etc., even at −70 °C in toluene. Therefore, ^{19}F NMR spectra of [B(C$_6$F$_5$)$_4$]$^-$ salts are unlikely to be reliable predictors of the degree to which the [B(C$_6$F$_5$)$_4$]$^-$ ion is associated with the cation. It also seems unlikely that one could distinguish between association of a [B(C$_6$F$_5$)$_4$]$^-$ ion with a cation in more than one position, i.e., on more than

(55) Waymouth, R. W.; Potter, K. S.; Schaefer, W. P.; Grubbs, R. H. *Organometallics* **1990**, *9*, 2843−2846.
(56) Waymouth, R. M.; Bronikowski, M. J.; Coots, R. J.; Grubbs, R. H.; Santarsiero, B. D. *J. Am. Chem. Soc.* **1986**, *108*, 1427.
(57) Waymouth, R. M.; Santarsiero, B. D.; Grubbs, R. H. *J. Am. Chem. Soc.* **1984**, *106*, 4050.
(58) Watson, P. L.; Parshall, G. W. *Acc. Chem. Res.* **1985**, *18*, 51.
(59) Stults, S. D.; Andersen, R. A.; Zalkin, A. *J. Am. Chem. Soc.* **1989**, *111*, 4507.
(60) Bochmann, M.; Lancaster, S. J. *Angew. Chem., Int. Ed. Engl.* **1994**, *33*, 1634.
(61) Beck, S.; Prosenc, M. H.; Brintzinger, H. H.; Goretzki, R.; Herfert, N.; Fink, G. *J. Mol. Catal. A* **1996**, *111*, 67.
(62) Koehler, K.; Piers, W. E.; Jarvis, A. P.; Xin, S.; Feng, Y.; Bravakis, A. M.; Collins, S.; Clegg, W.; Yap, G. P. A.; Marder, T. B. *Organometallics* **1998**, *17*, 3557.
(63) Bochmann, M.; Lancaster, S. J.; Hursthouse, M. B.; Malik, K. M. A. *Organometallics* **1994**, *13*, 2235.
(64) Jia, L.; Yang, X.; Stern, C. L.; Marks, T. J. *Organometallics* **1997**, *16*, 842.
(65) Yang, X.; Stern, C. L.; Marks, T. J. *Organometallics* **1991**, *10*, 840.
(66) Deck, P. A.; Beswick, C. L.; Marks, T. J. *J. Am. Chem. Soc.* **1998**, *120*, 1772.
(67) Vanka, K.; Chan, M. S. W.; Pye, C. C.; Ziegler, T. *Organometallics* **2000**, *19*, 1841.
(68) Deck, P. A.; Marks, T. J. *J. Am. Chem. Soc.* **1995**, *117*, 6128.

one type of pseudotetrahedral face of a cation; only one "free" isotropic $[B(C_6F_5)_4]^-$ ion is likely to be observed.

A plausible scenario is that **6b$_1$** is a tight ion pair in which the anion is weakly bound on the "apical" CNN face of the incipient trigonal-bipyramidal species, while **6b$_2$** is a related species in which the anion is associated more weakly with the cation on another tetrahedral face and bromobenzene is bound in the apical position through the lone pairs on the bromide. The process of converting **6b$_1$** to **6b$_2$** consists essentially of removing the $[B(C_6F_5)_4]^-$ ion from one pseudo-tetrahedral face of **6b**$^+$. The observed value of $\Delta G^{\ddagger}$ for that proposed process in bromobenzene at 298 K is ~14 kcal mol^{-1} ($\Delta H^{\ddagger} = 16.3(5)$ kcal mol^{-1} and $\Delta S^{\ddagger} = 8(2)$ cal mol^{-1} K^{-1}). This value is essentially the same as the estimated value for ΔH_{ips} in a metallocene cation in chlorobenzene.

We have also considered the possibility that **6b$_1$** is a dimeric dicationic version of **6b$_2$** (or vice versa) that contains two bridging methyl groups. In that circumstance a labeled methyl group might exchange between **6a** and **6b**. However, we do not observe any such exchange. Formation of a dimeric dication also would seem to be unlikely for steric reasons. Nevertheless, a dimeric dication is still a possible explanation.

There are some observations that cannot be explained readily. For example, the observation of more than one form of **6b$_2$** in dilute bromobenzene/toluene mixtures at low temperatures might be ascribed to formation of a toluene solvate as well as a bromobenzene solvate or to formation of C_1-symmetric "twisted" cations.

Why has a similar process not been observed in metallocene chemistry? In three-coordinate metallocene "cations" the process might be observable "indirectly" by methods employed to study migration of the $[MeB(C_6F_5)_3]^-$ ion from one position to another,[66,68] but to our knowledge no $[B(C_6F_5)_4]^-$ salts are stable enough to study in this manner.

We had hoped to determine whether more than one form of either an ether adduct or a dimethylaniline adduct could be observed at low temperatures. Unfortunately, these "strongly solvated", i.e., five-coordinate, species crystallize out of bromobenzene/toluene mixtures at low temperatures. There also is evidence for additional complications that revolve around the orientation of the base in the apical position, "twisting" of the ligand backbone, etc., as described in Results. In any case, we suspect that a crowded five-coordinate species would show little tendency to associate a $[B(C_6F_5)_4]^-$ anion strongly enough to allow different ion pairs to be observed at accessible temperatures.

The next step is to explore the behavior of all species discussed here in terms of olefin polymerization. We have established already that **2a** and **2b**, not surprisingly, are inactive for the polymerization of 1-hexene, while **3**, **5**, and **6** are all very active for polymerization of 1-hexene. We will be especially interested in whether living polymerization characteristics are compromised to varying degrees (and if so, how) as a consequence of a mixture of ion pairs being present. As one might imagine, which ion pairs are formed will be sensitive to virtually all parameters, including the size of the alkyl/growing polymer chain. The behavior of **5** as a catalyst will be especially interesting to explore, since inter alia it is a model for more complex "base adducts" of a cationic alkyl: i.e., in which the "base" is a main-group alkyl such as trimethylaluminum. Studies aimed in these directions are under way.

Experimental Section

Unless otherwise indicated, all manipulations were performed using standard Schlenk techniques or in a N_2-filled glovebox. Toluene, diethyl ether, and pentane were sparged with N_2 and then passed though columns of activated alumina. THF was distilled from sodium−benzophenone ketyl. Solvents were stored in the glovebox over activated 4 Å molecular sieves. Chlorobenzene (HPLC grade) and deuterated solvents were sparged with N_2 and stored over activated 4 Å molecular sieves for 2 days prior to use. Chemical shifts are reported in ppm relative to TMS (^{1}H, and ^{13}C) or external $CFCl_3$ in $CDCl_3$ (^{19}F) at room temperature, unless otherwise indicated; *J* values are given in Hz. All nonobvious resonances have been assigned on the basis of ^{1}H gCOSY, ^{1}H ROESY (typically with 60 to 300 ms mixing time), ^{13}C{^{1}H} DEPT, and ^{1}H−^{13}C HMQC. Some resonances in ^{13}C spectra are not listed. The temperature of the NMR probe was obtained by standardization with methanol or ethylene glycol. Quantitative line-shape analysis (LSA) was carried out using gNMR V3.6.5 software (Peter H. M. Budzelaar, IvorySoft 1992: Palo Alto, CA). High-resolution MS was recorded on a Finnigan MAT 8200 Sector mass spectrometer. Elemental analyses were performed by H. Kolbe, Mikroanalytisches Laboratorium (Mühlheim an der Ruhr, Germany). X-ray data were collected on a Bruker CCD diffractometer with λ(Mo Kα) = 0.710 73 Å and solved using a full-matrix least-squares refinement on F^2. Grignard reagents and organolithium reagents were prepared in the normal fashion and titrated with 2-butanol in the presence of 1,10-phenanthroline prior to use.

(MesNHCH$_2$CH$_2$)$_2$NH (H$_2$[N$_2$NH]). A 2 L Schlenk flask was charged with diethylenetriamine (23.450 g, 0.227 mol), mesityl bromide (90.51 g, 0.455 mol), tris(dibenzylideneacetone)dipalladium(0) (1.041 g, 1.14 mmol), rac-2,2′-bis(diphenylphosphino)-1,1′-binaphthyl (2.123 g, 3.41 mmol), sodium *tert*-butoxide (65.535 g, 0.682 mol), and toluene (800 mL). The reaction mixture was heated to 95 °C in an oil bath and stirred for 4 days. All solvent was removed in vacuo at ~50 °C to leave a dark brown solid residue. The residue was dissolved in diethyl ether (1 L), and the solution was washed three times with water (1 L) and saturated aqueous NaCl (0.5 L) and dried over magnesium sulfate. Removal of the ether in vacuo left a red oil, which was further heated at 70 °C overnight (~12 h) at 40 mTorr. The red oil crystallized upon cooling to room temperature to give red needlelike crystals; yield 71.10 g, 92%. The red crystals were pure, as judged by ^{1}H NMR, and were used in subsequent reactions. The product was recrystallized from pentane to afford yellow crystals; yield 65.45 g (85%): ^{1}H NMR (C_6D_6) δ 6.83 (s, 4, Ar), 3.39 (br s, 2, ArN*H*), 2.86 (t, 4, CH_2), 2.49 (t, 4, CH_2), 2.27 (s, 12, Me_o), 2.21 (s, 6, Me_p), 0.68 (br s, 1, CH_2NHCH_2); ^{13}C NMR (C_6D_6) δ 143.74 (C, Ar), 131.35 (C, Ar), 129.83 (C, Ar), 129.55 (CH, Ar), 50.17 (CH_2), 48.56 (CH_2), 20.70 (Me_p), 18.51 (Me_o); IR ($CHCl_3$) cm^{-1} 3357 (NH stretch, medium); high-resolution MS (EI, 70 eV) 339.267 32 (calcd 339.267 448). Anal. Calcd for $C_{22}H_{33}N_3$: C, 77.83; H, 9.80; N; 12.38. Found: C, 77.85; H, 9.72; N, 12.31.

(MesNHCH$_2$CH$_2$)$_2$NMe (H$_2$[N$_2$NMe]). A 250 mL Schlenk flask was charged with H_2[N_2NH] (10.0 g, 29.45 mmol), K_2CO_3 (15 g), and acetonitrile (100 g). This solution was cooled to 0 °C, and MeI (1.9 mL, 30.52 mmol) was added. The solution was warmed to room temperature and was stirred for 20 h. The reaction mixture was extracted with pentane/water (100 mL/100 mL) in air. The pentane layer was separated, and the water was washed with pentane (2 × 50 mL). The organic phases were combined, and the solvent was removed in vacuo; yield 8.43 g (81%): ^{1}H NMR (300 MHz, $CDCl_3$) δ 7.04 (s, 4, C*H*), 3.29 (t, 4, J_{HH} = 6.6, CH_2), 2.84 (t, 4, J_{HH} = 6.6, CH_2),

2.50 (s, 12, CH_3), 2.48 (s, 3, NCH_3), 2.45 (s, 6, CH_3); ^{13}C NMR (121 MHz, $CDCl_3$) δ 143.91 (Ar), 130.79 (Ar), 129.47 (Ar), 129.24 (Ar), 58.41 (CH_2), 46.09 (CH_2), 41.42 (NCH_3), 20.57 (CH_3), 18.49 (CH_3).

[N$_2$NH]Zr(NMe$_2$)$_2$. Solid Zr(NMe$_2$)$_4$ (3.12 g, 11.7 mmol) was added to a slurry of H$_2$[N$_2$NH] (4.1 g, 12.1 mmol) in 20 mL of pentane. The solution was stirred for 24 h. The precipitated product was filtered off, washed with cold pentane (2 × 10 mL), and dried in vacuo; yield 3.56 g, 59%: ^{1}H NMR (C_6D_6) δ 6.96 (s, 2, Ar), 6.95 (s, 2, Ar), 3.36 (m, 2, CH_2), 3.05 (s, 6, NMe), 3.01 (m, 2, CH_2), 2.61 (m, 4, CH_2), 2.47 (s, 6, Me$_o$), 2.45 (s, 6, Me$_p$), 2.28 (s, 6, NMe), 2.21 (s, 6, Me$_o$), 1.80 (br s, 1, NH); ^{13}C NMR (C_6D_6) δ 150.48 (C, Ar), 134.49 (C, Ar), 132.06 (C, Ar), 129.61 (CH, Ar), 55.59 (CH_2), 49.26 (CH_2), 44.62 (NMe), 41.27 (NMe), 21.31 (Me$_p$), 19.52 (Me$_o$). Anal. Calcd for $C_{26}H_{43}N_5Zr$: C, 60.42; H, 8.39; N; 13.55. Found: C, 60.31; H, 8.29; N, 13.39.

[N$_2$NMe]Zr(NMe$_2$)$_2$. Solid Zr(NMe$_2$)$_4$ (3.10 g, 11.59 mmol) was added to a solution of H$_2$[N$_2$NMe] (4.10 g, 11.59 mmol) in 20 mL of pentane. The solution was stirred for 24 h and filtered. The solid product was washed with pentane and dried; yield 4.24 g (69%): ^{1}H NMR (300 MHz, C_6D_6) δ 6.95 (s, 4, CH), 3.41 (m, 2, CH_2), 3.10 (2, 6, N(CH_3)$_2$), 3.20 (m, 2, CH_2), 2.78 (m, 2, CH_2), 2.49 (s, 6, CH_3), 2.51 (s, 6, N(CH_3)$_2$), 2.37 (s, 6, CH_3), 2.33 (m, 2, CH_2), 2.22 (s, 3, NCH_3), 2.21 (s, 6, CH_3).

[N$_2$NH]ZrCl$_2$. $(CH_3)_3SiCl$ (0.66 mL, 5.16 mmol) was added to a solution of [N$_2$NH]Zr(NMe$_2$)$_2$ (1.21 g, 2.33 mmol) in 20 mL of diethyl ether. The reaction mixture was stirred for ~16 h. The precipitated product was filtered off and washed with pentane; yield 1.07 g (92%): ^{1}H NMR δ 6.88 (s, 2, Ar), 6.83 (s, 2, Ar), 3.32 (m, 2, CH_2), 2.86 (m, 2, CH_2), 2.50 (s, 6, Me$_o$), 2.45 (m, 4, CH_2), 2.40 (s, 6, Me$_o$), 2.20 (br s, 1, NH), 2.13 (s, 6, Me$_p$); ^{13}C NMR δ 146.28 (C, Ar), 135.52 (C, Ar), 134.48 (C, Ar), 134.14 (C, Ar), 130.48 (CH, Ar), 130.28 (CH, Ar), 57.13 (CH_2), 49.43 (CH_2), 21.33 (Me$_p$), 19.49 (Me$_o$), 19.41 (Me$_o$). Anal. Calcd for $C_{22}H_{31}Cl_2N_3Zr$: C, 52.89; H, 6.25; N; 8.41. Found: C, 52.76; H, 6.35; N, 8.48.

[N$_2$NMe]ZrCl$_2$. $(CH_3)_3SiCl$ (4.0 mL, 31.3 mmol) was added to a solution of [N$_2$NMe]Zr(NMe$_2$)$_2$ (4.12 g, 7.76 mmol) in 50 mL of diethyl ether. The reaction mixture was stirred for 24 h. The precipitated product was filtered off and washed with pentane (40 mL); yield 3.52 g (88%).

[N$_2$NH]ZrMe$_2$ (1a). Method A. Methylmagnesium iodide (0.1 mL, 3 M in diethyl ether, 2 equiv) was added to a cold solution (−30 °C) of [N$_2$NH]ZrCl$_2$ (75 mg, 0.150 mmol) in diethyl ether (5 mL). The reaction mixture was slowly warmed to room temperature and stirred for 10 min. Proton NMR revealed that the product had formed cleanly. Dioxane (5 drops) was added, and the precipitate was removed via filtration. The filtrate was concentrated in vacuo to ~1 mL. Pentane (2 mL) was added to the concentrated filtrate in order to precipitate white solid product; yield 69 mg (76%).

Method B. Solid $ZrCl_4$ (0.709 g, 0.304 mmol) was added in portions to a diethyl ether solution (20 mL) of H$_2$[N$_2$NH] (1.033 g, 0.304 mmol) at −30 °C with vigorous stirring. The solution was warmed and stirred at room temperature. Pale yellow solid precipitated gradually over a period of 1 h. The yellow suspension was cooled to −30 °C, and methylmagnesium iodide (4.1 mL, 3 M in diethyl ether, 4.1 equiv) was added. Gas evolved and the solution immediately turned white and cloudy. The solution was stirred at room temperature for 10 min, and then 1,4-dioxane (1.2 g, 4.5 equiv) was added. The reaction mixture was filtered through Celite, which was washed with diethyl ether (2 × 10 mL). The pale yellow solution was concentrated in vacuo to ~20 mL and chilled to −30 °C for 1 h to give colorless crystals; yield (3 crops) 0.571 g (41%).

Method C. H$_2$[N$_2$NH] (10.798 g, 31.8 mmol) was dissolved in 250 mL of toluene in a 500 mL round-bottom flask. $ZrCl_4$ (7.411 g, 31.8 mmol) was added as a solid, and the mixture was heated to 80 °C and stirred for 24 h. The mixture was cooled to room temperature, and 43.5 mL of MeMgBr (3.0 M in ether, 130.3 mmol) was added dropwise with stirring over 30 min. The mixture was stirred for 60 min, and MgClBr was filtered off. The toluene and ether were removed under vacuum, and the solids were extracted with toluene (200 mL). The mixture was filtered and the volume of toluene was reduced to 10 mL. Pentane (250 mL) was added, which induced precipitation of a pale brown solid. The solid product was isolated by filtration, washed with 50 mL of cold pentane, and dried under vacuum; yield 15.20 g (86%): ^{1}H NMR (C_6D_6) δ 6.99 (s, 2, Ar), 6.97 (s, 2, Ar), 3.31 (m, 2, CH_2), 3.13 (m, 2, CH_2), 2.53 (s, 6, Me$_o$), 2.43 (s, 6, Me$_o$), 2.36 (m, 4, CH_2), 2.21 (s, 6, Me$_p$), 1.16 (br s, 1, NH), 0.24 (s, 3, ZrMe$_{eq}$), 0.07 (s, 3, ZrMe$_{ax}$); ^{13}C NMR (C_6D_6) δ 146.56 (C, Ar), 136.07 (C, Ar), 135.55 (C, Ar), 134.23 (C, Ar), 130.29 (CH, Ar), 129.98 (CH, Ar), 57.46 (CH_2), 51.27 (CH_2), 42.45 (ZrMe$_{eq}$), 39.63 (ZrMe$_{ax}$), 21.44 (Me$_p$), 19.39 (Me$_o$), 19.28 (Me$_o$). Anal. Calcd for $C_{24}H_{37}N_3Zr$: C, 62.83; H, 8.13; N; 9.16. Found: C, 62.91; H, 8.02; N, 9.04. Single crystals of [N$_2$NH]ZrMe$_2$ were grown from a mixture of diethyl ether, toluene, and hexamethyldisiloxane at −30 °C.

[N$_2$NH]Zr(^{13}CH$_3$)$_2$. To a stirred suspension of [N$_2$NH]ZrCl$_2$ (1.00 g, 2.00 mmol) in diethyl ether (30 mL) at −30 °C was added $^{13}CH_3MgI$ (2.3 M in Et$_2$O, 1.84 mL, 4.2 mmol). The mixture was stirred for 20 min without further cooling. The solvent was then removed in vacuo and the residue dissolved in toluene (30 mL). This solution was then treated with 1,4-dioxane (680 mg, 7.71 mmol), which led to formation of a white precipitate. The slurry was filtered through Celite, and the solvent was removed from the filtrate in vacuo, yielding ^{13}C-labeled **1a**; yield 0.54 g (58%). The product can be recrystallized from a mixture of ether and pentane at −30 °C: ^{1}H NMR (C_6D_6) δ 6.99 (s, 2, CH), 6.97 (s, 2, CH), 3.33 (m, 2, CHH), 3.12 (m, 2, CHH), 2.53 (s, 6, *p*-CH_3), 2.43 (s, 6, *o*-CH_3), 2.36 (m, 4, CHH), 2.21 (s, 6, *o*-CH_3), 1.2 (m, NH), 0.23 (d, J_{CH} = 136, Zr^{13}CH_3), 0.07 (d, J_{CH} = 135, Zr^{13}CH_3); ^{13}C NMR (C_6D_6) δ 42.49 (ZrCH_3), 39.43 (ZrCH_3).

[N$_2$NMe]ZrMe$_2$ (1b). Method A. Methyllithium (0.15 mL, 1.4 M in Et$_2$O, 0.21 mmol) was added to a slurry of [N$_2$NH]-ZrMe$_2$ (0.098 g, 0.21 mmol) in Et$_2$O (3 mL) at −30 °C. The white slurry immediately turned pale yellow, and the mixture became homogeneous. The solution was warmed and stirred at room temperature for 1 h and then chilled to −30 °C. Methyl iodide (0.045 g, 0.32 mmol, 1.5 equiv) was added to the cold solution, and the reaction mixture was stirred at room temperature for 1 h. All volatile components were removed in vacuo, and the solid residue was extracted with toluene (5 mL). Toluene was removed from the extract in vacuo, and the residue was redissolved in pentane (10 mL). The volume of the solution was reduced in vacuo to ~2 mL to afford a colorless crystalline solid. The concentrated solution was kept at −30 °C for 2 h, and the crystalline product was collected; yield 64 mg (63%).

Method B. To 10.00 g of {H$_2$[N$_2$NH]}ZrCl$_4$ (17.4 mmol) (prepared from H$_2$[N$_2$NH] and $ZrCl_4$ in toluene) suspended in 250 mL of Et$_2$O in a 500 mL round-bottom flask at −40 °C was added dropwise 65.5 mL of MeLi (1.4 M, 91.7 mmol) over 30 min with stirring. The mixture was warmed to room temperature and stirred for 30 min. The mixture was cooled to −40 °C, and 3.14 g of MeI (22.1 mmol) in 5 mL ether was added dropwise with stirring over 5 min. The mixture was warmed to room temperature, and the ether was removed in vacuo. The product was extracted with toluene (250 mL), and the extract was filtered to remove LiCl and LiI. The filtrate volume was reduced to 30 mL in vacuo, and 250 mL of pentane was added, causing precipitation of a pale brown solid. The solid product was isolated by filtration, washed with 50 mL of cold pentane, and dried under vacuum; yield 7.82 g (95%).

Method C. A slurry of [N$_2$NMe]ZrCl$_2$ (1.02 g, 1.99 mmol) in 20 mL of Et$_2$O was cooled to −20 °C. This mixture was then treated with MeMgBr (1.5 mL, 3 M in Et$_2$O, 4.5 mmol). The slurry became homogeneous, and a solid precipitated. The mixture was stirred for 10 min, and then all solvents were removed in vacuo. The residue was dissolved in 20 mL of

toluene, and 0.5 mL of 1,4-dioxane was added. The solution was stirred for 10 min and then filtered through Celite. The solvent was removed from the filtrate in vacuo; yield 0.89 g (95%): ^{1}H NMR δ 6.99 (s, 2, Ar), 6.95 (s, 2, Ar), 3.62 (m, 2, CH_2), 2.98 (m, 2, CH_2), 2.66 (m, 2, CH_2), 2.47 (s, 6, Me_p), 2.44 (s, 6, Me_o), 2.20 (s, 6, Me_o), 2.12 (m, 2, CH_2), 2.01 (s, 3, NMe), 0.26 (s, 3, $ZrMe_{eq}$), 0.23 (s, 3, $ZrMe_{ax}$); ^{13}C NMR δ 146.13 (C, Ar), 136.63 (C, Ar), 136.08 (C, Ar), 134.32 (C, Ar), 130.36 (CH, Ar), 130.05 (CH, Ar), 61.14 (CH_2), 55.89 (CH_2), 43.31 (ZrMe), 40.62 (ZrMe), 37.10 (NMe), 21.42 (Me_p), 19.20 (Me_o), 19.09 (Me_o). Anal. Calcd for $C_{25}H_{39}N_3Zr$: C, 63.51; H, 8.31; N; 8.89. Found: C, 63.26; H, 8.14; N, 8.85. X-ray-quality crystals were grown from a mixture of ether and pentane at −30 °C.

[N_2N(*CH_3)]Zr(#CH_3)$_2$. To a stirred suspension of [N_2NH]-Zr($^{13}CH_3$)$_2$ (0.43 g, 0.933 mmol) in Et_2O (15 mL) at −30 °C was added a 1.6 M solution of LiMe in Et_2O (0.60 mL, 0.96 mmol). The resulting pale yellow cloudy solution that formed was stirred for 20 min while the temperature was allowed to increase to room temperature. The solution was then cooled to −30 °C, and $^{13}CH_3I$ (85 μL, 1.4 mmol) was added dropwise. The mixture was stirred for 30 min. The solvent was removed in vacuo, and the residue was extracted with toluene. The toluene was removed in vacuo, leaving a crystalline tan solid, which was washed with cold pentane (4 mL) and dried in vacuo; yield 0.38 g (81%): ^{1}H NMR (300 MHz, C_6D_6/C_6D_5Br) δ 6.92/6.87 (s, 2, C*H*), 6.45/6.85 (s, 2, C*H*), 3.62/3.71 (m, 2, CH*H*), 2.90/3.05 (m, 2, CH*H*), 2.65/2.93 (m, 2, CH*H*), 2.47/2.39 (s, 6, *p*-CH_3), 2.44/2.34 (s, 6, *o*-CH_3), 2.20/2.14 (s, 6, *o*-CH_3), 2.15/2.14 (m, 2, CH*H*), 2.01/2.29 (d, J_{CH} = 136.3, N^{13}CH_3), 0.26/0.03 (s, d, 3, J_{CH} = 114, Zr$^{2/3\times13}$CH_3), 0.24/-0.05 (s, d, 3, J_{CH} = 114, Zr$^{2/3\times13}$CH_3); ^{13}C NMR (121 MHz, C_6D_6/C_6D_5Br) δ 43.31/42.52 (s, ZrCH_3), 40.63/39.89 (s, Zr*C*H$_3$), 37.09/36.78 (s, N*C*H$_3$).

{**[N_2NH]ZrMe(Et_2O)**}**[$B(C_6F_5)_4$] (2a).** A solution of [Ph_3C]-[$B(C_6F_5)_4$] (0.25 g, 0.27 mmol) in PhCl (3 mL) at −30 °C was added to a solution of **1a** (0.13 g, 0.75 mmol) in PhCl (3 mL) at −30 °C. The resulting orange solution was stirred for 5 min, and then Et_2O (1 mL) was added. The solution was filtered, and the filtrate was evaporated to dryness in vacuo. The waxy red residue was triturated with pentane (5 mL), leaving a yellow powder which was washed with pentane (3 × 10 mL) and then vacuum-dried; yield 0.28 g (86%): ^{1}H NMR (500 MHz, C_6D_5Br) δ 6.79 (s, 2, C*H*), 6.72 (s, 2, C*H*), 3.41 (m, 2, CH*H*), 3.15 (m, 2, CH*H*), 2.97 (m, 2, CH*H*), 2.82 (m, 2, CH*H*), 2.77 (q, 4, J_{HH} = 6.9, °CH_2), 2.19 (s, 6, *p*-CH_3), 2.13 (s, 6, *o*-CH_3), 1.91 (s, 6, *o*-CH_3), 1.03 (m, N*H*), 0.25 (t, 6, J_{HH} = 6.9, CH_2CH_3), 0.13 (s, 3, ZrCH_3); ^{19}F (471 MHz, C_6D_5Br) δ −132.16 (br, 2, *o*-C*F*), −162.20 (t, 1, *J* = 21.4, *p*-C*F*), −166.20 (broad, 2, *m*-C*F*). Anal. Calcd for $C_{51}H_{44}BF_{20}N_3OZr$: C, 51.80; H, 3.71; N, 4.51. Found: C, 51.64; H, 3.82; N, 4.37.

{**[N_2NMe]ZrMe(Et_2O)**}**[$B(C_6F_5)_4$] (2b).** Complex **2b** was prepared from **1b** (0.24 g, 0.508 mmol) and [Ph_3C][$B(C_6F_5)_4$] (0.47 g, 0.508 mmol) in PhCl (5 mL) by following the procedure described for **2a**; yield 0.56 g (92%): ^{1}H NMR (500 MHz, C_6D_5-Br) δ 6.79 (s, 2, C*H syn* with respect to NCH$_3$), 6.72 (s, 2, C*H*), 3.42 (m, 2, CH*H*), 3.18 (m, 2, CH*H*NCH$_3$), 2.98 (m, 2, CH*H*), 2.79 (q, 4, J_{HH} = 6.9, OCH_2), 2.65 (m, 2, CH*H*NCH$_3$), 2.38 (s, 3, J_{CH} = 138, NCH_3), 2.39 (s, 6, *o*-CH_3 *syn* with respect to NCH$_3$), 2.13 (s, 6, *o*-CH_3), 1.93 (s, 6, *o*-CH_3), 0.22 (t, 6, J_{HH} = 138, 6.9, CH_2CH_3), 0.19 (s, 3, J_{CH} = 115.3, ZrCH_3); ^{13}C NMR (126 MHz, C_6D_5Br) δ 149.0 (*C*), 137.7 (*C*), 135.8 (*C*), 134.5 (*C*), 130.6 (*C*H *syn* with respect to NCH$_3$), 130.2 (*C*H), 67.79 (O*C*H$_2$), 57.54 (*C*H$_2$), 53.83 (*C*H$_2$NCH$_3$), 45.69 (N*C*H$_3$), 39.81 (Zr*C*H$_3$), 20.58 (*o*-*C*H$_3$ *syn* with respect to NCH$_3$), 18.28 (*p*-*C*H$_3$), 17.99 (*o*-*C*H$_3$), 11.78 (CH$_2$*C*H$_3$); ^{19}F (471 MHz, C_6D_5Br): δ −132.08 (broad, 2, *o*-C*F*), −162.41 (t, 1, *J* = 21.4, *p*-C*F*), −166.28 (broad, 2, *m*-C*F*). Anal. Calcd for $C_{52}H_{46}BF_{20}N_3OZr$: C, 51.58; H, 3.83; N, 3.47. Found: C, 51.68; H, 3.92; N, 3.41. Crystals of **2b** suitable for X-ray diffraction were grown from pentane/chlorobenzene at −25 °C. The ^{13}C-labeled complex was prepared from ^{13}C-labeled **1b** by following an identical procedure.

{**[N_2NMe]Zr(CH_3)(NMe_2Ph)**}**[$B(C_6F_5)_4$] (3b).** To a solution of [N_2NMe]Zr(CH_3)$_2$ (0.20 g, 0.42 mmol) in chlorobenzene (8 mL) at −30 °C was added [NMe_2Ph][$B(C_6F_5)_4$] (0.34 g, 0.42 mmol). The resulting orange solution was stirred for 90 min, filtered, and evaporated to dryness. The resulting orange oil was vigorously stirred with pentane (5 mL), yielding {[N_2NMe]-Zr(CH_3)(NMe_2Ph)}[$B(C_6F_5)_4$] as an orange powder which was washed with pentane (3 × 15 mL) and vacuum-dried; yield 0.53 g (98%): ^{1}H NMR (300 MHz, C_6D_5Br) δ 6.81 (s, 2, CH *syn* with respect to NCH$_3$), 6.78 (s, 2, CH), 6.42 (broad, H, anil-*p*-CH), 6.29 (broad, 2, anil-*m*-CH), 5.66 (d, 2, J_{HH} = 8.5, anil-*o*-CH), 3.29 (m, 2, CHH), 2.97 (m, 2, CHH), 2.92 (m, 2, CHH), 2.58 (m, 2, CHH), 2.40 (s, 3, J_{HC} = 138, NCH$_3$), 2.32 (broad, 6, PhNCH$_3$), 2.20 (s, 6, *p*-CH$_3$), 2.13 (s, 6, *o*-CH$_3$ *syn* with respect to NCH$_3$), 1.89 (s, 6, *o*-CH$_3$), 0.07 (broad, 3, J_{CH} = 119, ZrCH$_3$); ^{13}C NMR (126 MHz, C_6D_5Br) δ 130.3 (*C*H *syn* with respect to NCH$_3$), 130.2 (*C*H), 56.7 (*C*H$_2$), 55.3 (*C*H$_2$), 46.47 (N*C*H$_3$), 37.0 (broad, Zr*C*H$_3$), 20.72 (*p*-*C*H$_3$), 18.49 (*o*-*C*H$_3$ *syn* with respect to NCH$_3$), 17.73 (*o*-*C*H$_3$); ^{19}F (471 MHz, C_6D_5Br) δ −131.71 (broad, 2, 2-C*F*), −162.03 (t, 1, J_{FF} = 2124, 4-C*F*), −165.88 (broad, 2, 3-C*F*). Anal. Calcd for $C_{56}H_{47}N_4BF_{20}Zr$: C, 53.47; H, 3.77; N, 4.45. Found: C, 53.56; H, 3.69; N, 4.41. The ^{13}C-labeled complexes were prepared by identical procedures.

Preparation of Impure {[{[2-(CH_2)-4,6-(CH_3)$_2$$C_6H_2$]N-$CH_2CH_2$}N($CH_2CH_2$NMes)($CH_3$)]Zr(N$Me_3$Ph)}[$B(C_6F_5)_4$] (4b). To a solution of [N_2NMe]Zr(CH_3)$_2$ (0.10 g, 0.21 mmol) in chlorobenzene (2 mL) at −30 °C was added a suspension of [NMe_2Ph][$B(C_6F_5)_4$] (0.17 g, 0.21 mmol) in chlorobenzene (2 mL), also at −30 °C. The resulting orange solution was stirred for 1 h, filtered, and evaporated to dryness. The resulting foamy residue was treated with pentane (5 mL) to afford the product as an off-yellow powder, which was washed with pentane (3 × 10 mL) and vacuum-dried; yield 0.25 g (95%): ^{1}H NMR (500 MHz, C_6D_5Br) δ 6.92 (s, 1, C*H*), 6.77 (m, 1, anil-*p*-C*H*), 6.76 (m, 2, anil-*m*-C*H*), 6.72 (s, 1, C*H*), 6.71 (s, 1, 5-C*H*), 6.08 (s, 1, 3-C*H*), 5.75 (d, 2, J_{HH} = 7.5, anil-*o*-C*H*), 4.34 (m, 1, CH*H*), 3.81 (m, 1, CH*H*), 3.23 (m, 1, CH*H*), 3.02 (m, 1, CH*H*), 2.78 (m, 1, CH*H*), 2.70 (m, 1, CH*H*), 2.60 (m, 1, CH*H*), 2.55 (m, 1, CH*H*), 2.53 (s, 3, NCH_3), 2.39 (d, 1, J_{HH} = 12.5, ZrCH*H*), 2.24 (s, 3, *o*-CH_3), 2.21 (s, 3, *p*-CH_3), 2.18 (s, 3, 9-CH_3), 2.09 (s, 3, anil-NCH_3), 2.06 (s, 3, 8-CH_3), 1.92 (s, 3, *o*-CH_3), 1.91 (s, 3, anil-NCH_3), 0.79 (d, 1, J_{HH} = 12.5, ZrCH*H*); ^{13}C NMR (121 MHz, C_6D_5Br) δ 132 (s, *C*H anil), 130.55 (*C*H), 130.02 (*C*H), 129.95 (5-*C*H), 126.78 (3-*C*H), 114.18 (anil-*o*-*C*H), 68.90 (Zr*C*H$_2$), 65.32 (N*C*H$_2$), 60.29 (N*C*H$_2$), 55.76 (N*C*H$_2$), 54.70 (N*C*H$_2$), 46.53 (anil-N*C*H$_3$), 42.23 (anil-N*C*H$_3$), 40.43 (N*C*H$_3$), 20.79 (9-*C*H$_3$), 20.65 (*p*-*C*H$_3$), 19.29 (8-CH3), 18.94 (o-CH$_3$), 18.64 (o-CH$_3$).

[{[N_2NMe]Zr(CH_3)}$_2$(μ-CH_3)][$B(C_6F_5)_4$] (5b). To a solution of [Ph_3C][$B(C_6F_5)_4$] (0.15 g, 0.16 mmol) in chlorobenzene (3 mL) at −30 °C was added a solution of [N_2NMe]Zr(CH_3)$_2$ (0.15 g, 0.32 mmol) in chlorobenzene (3 mL) at −30 °C. The resulting pale yellow solution was stirred for 15 min at ∼20 °C. The solution was then added dropwise to pentane (60 mL), yielding **5b** as an off-white precipitate. The product was separated by filtration, washed with pentane (2 × 3 mL), and vacuum-dried; yield 0.23 g (87%): ^{1}H NMR (500 MHz, −25 °C, C_6D_5Br) δ 6.95 (s, 2, C*H syn* with respect to NCH$_3$), 6.88 (s, 2, C*H*), 6.80 (s, 2, C*H syn* with respect to NCH$_3$), 6.75 (s, 2, C*H*), 3.26 (m, 2, CH*H*), 3.19 (m, 2, CH*H*), 2.99 (m, 2, CH*H*), 2.94 (m, 2, CH*H*), 2.64 (m, 4, CH*H*), 2.34 (m, 4, CH*H*), 2.32 (s, 6, *p*-CH_3), 2.28 (s, 6, *p*-CH_3), 2.23 (s, 6, *o*-CH_3 *syn* with respect to NCH$_3$), 2.19 (s, 6, *o*-CH_3 *syn* with respect to NCH$_3$), 2.11 (s, 6, NCH_3), 1.65 (s, 6, *o*-CH_3), 1.42 (s, 6, *o*-CH_3), −0.38 (s, 6, J_{CH} = 115, ZrCH_3), −0.89 (s, 3, J_{CH} = 133, ZrCH_3Zr); ^{13}C NMR (126 MHz, −25 °C, C_6D_5Br) δ 45.02 (s, NCH$_3$), 41.23 (s, ZrCH$_3$), 40.11 (s, ZrCH$_3$Zr); ^{1}H NMR (500 MHz, 20 °C, C_6D_5Br) δ 6.89 (broad, 4, C*H*), 6.82 (broad, 4, C*H syn* with respect to NCH$_3$), 3.27 (m, 4, CH*H*), 3.01 (m, 4, CH*H*), 2.72 (m, 4, CH*H*), 2.40 (m, 4, CH*H*), 2.28 (s, 12, *p*-CH_3), 2.21 (s, 12, *o*-CH_3 *syn* with respect to NCH$_3$), 2.18 (s, 6, NCH_3), 1.58 (broad, 12, *o*-CH_3), −0.36 (s, 6,

J_{CH} = 115, ZrCH_3), −0.85 (s, 3, J_{CH} = 133, ZrCH_3Zr); ^{13}C NMR (126 MHz, 20 °C, C_6D_5Br) δ 45.12 (s, NCH_3), 41.62 (s, ZrCH_3), 40.15 (s, ZrCH_3Zr); ^{19}F (471 MHz, 20 °C, C_6D_5Br) δ −131.65 (broad, 2, *o*-C*F*), −162.10 (t, 1, *J* = 21.2, *p*-C*F*), −165.92 (broad, 2, *m*-C*F*). Anal. Calcd for $C_{73}H_{75}BF_{20}N_6Zr_2$: C, 54.47; H, 4.70; N, 5.22. Found: C, 54.55; H, 4.76; N, 5.09. Single crystals of [{[N_2NMe]Zr(CH_3)}$_2$(μ-CH_3)][B(C_6F_5)$_4$] suitable for X-ray diffraction were grown from a mixture of toluene and chlorobenzene at −25 °C.

Observation of {[N_2NH]Zr(CH_3)}[B(C_6F_5)$_4$] (6a$_2$). To a solution of **1a** (0.02 g, 46 μmol) in C_6D_5Br (0.4 mL) at −30 °C was added a solution of [Ph_3C][B(C_6F_5)$_4$] (0.04 g, 46 μmol) in C_6D_5Br (0.4 mL), also at −30 °C. The resulting orange solution was transferred to an NMR tube: ^{1}H NMR (500 MHz, −25 °C, C_6D_5Br) δ 6.82 (s, 4, C*H*), 3.07 (m, 2, CH*H*), 2.90 (m, 2, CH*H*), 2.81 (s, N*H*), 2.70 (m, 2, CH*H*), 2.66 (m, 2, CH*H*), 2.23 (s, 6, *p*-CH_3 *syn* to NH), 2.04 (s, 6, *o*-CH_3), 1.97 (s, 6, *o*-CH_3 *syn* to NCH_3), −0.13 (s, 3, J_{CH} = 117, ZrCH_3); ^{1}H NMR (500 MHz, 20 °C, C_6D_5Br) δ 6.82 (br, 4, C*H*), 3.13 (br, 4, CH*H*), 2.78 (m, 4, CH*H*), 2.7 (br, N*H*), 2.21 (br, 6, *p*-CH_3), 2.03 (br, 6, *o*-CH_3), 1.98 (br, 6, *o*-CH_3), −0.08 (s, 3, J_{CH} = 117, ZrCH_3); ^{13}C NMR (126 MHz, −25 °C, C_6D_5Br) δ 31.29 (br, ZrCH_3); ^{13}C NMR (126 MHz, 20 °C, C_6D_5Br) δ 31.7 (br, ZrCH_3). The ^{13}C-labeled complex {[N_2NH]Zr(^{13}CH_3)}$^+$ was prepared from ^{13}C-labeled **1a** by the same procedure.

Observation of {[N_2NMe]Zr(CH_3)}[B(C_6F_5)$_4$] (6b$_1$/6b$_2$). To a solution of **1b** (20 mg, 42 μmol) in C_6D_5Br (0.4 mL) at −30 °C was added a solution of [Ph_3C][B(C_6F_5)$_4$] (39 mg, 42 μmol) in C_6D_5Br (0.4 mL), also at −30 °C. The resulting orange solution was transferred to an NMR tube. ^{1}H NMR of **6b$_2$** (500 MHz, −25 °C, C_6D_5Br): δ 6.66 (s, 2, C*H*), 6.65 (m, 2, C*H*), 3.45 (m, 2, CH*H*), 3.29 (m, 2, CH*H*), 2.98 (m, 2, CH*H*), 2.67 (m, 2, CH*H*), 2.32 (s, J_{CH} = 139, NCH_3), 2.16 (s, 6, *o*-CH_3 *syn* to NCH_3), 2.10 (s, 6, *p*-CH_3), 1.88 (s, 6, *o*-CH_3), 0.15 (s, J_{CH} = 115, ZrCH_3). ^{13}C NMR of **6b$_2$** (126 MHz, −25 °C, C_6D_5Br): δ 47.24 (s, ZrCH_3), 45.57 (s, NCH_3). ^{1}H NMR of **6b$_1$** (500 MHz, −25 °C, C_6D_5Br): δ 6.82 (s, 4, C*H*), 3.13 (m, 2, CH*H*), 2.78 (br, 4, CH*H*), 2.41 (br, 2, CH*H*), 2.29 (s, J_{CH} = 139, NCH_3), 2.23 (s, 6, *p*-CH_3), 2.08 (s, 6, *o*-CH_3), 2.02 (s, 6, *o*-CH_3 *syn* to NCH_3), −0.01 (s, 3, J_{CH} = 117, ZrCH_3). ^{13}C NMR of **6b$_1$** (126 MHz, −25 °C, C_6D_5Br): δ 46.51 (s, NCH_3), 33.52 (s, ZrCH_3). ^{19}F of **6b$_1$** (471 MHz, −25 °C, C_6D_5Br): δ −132.04 (br, 2, *o*-C*F*), −161.38 (br, 1, *p*-C*F*), −165.37 (br, 2, *m*-C*F*). ^{1}H NMR of **6b$_1$** (500 MHz, 20 °C, C_6D_5Br): δ 6.70 (s, 4, C*H*), 3.53 (m, 2, CH*H*), 3.34 (m, 2, CH*H*), 3.05 (m, 2, CH*H*), 2.73 (m, 2, CH*H*), 2.38 (s, 3, J_{CH} = 138, NCH_3), 2.18 (br s, 6, *o*-CH_3), 2.01 (br, 6, *p*-CH_3), 1.90 (br, 6, *o*-CH_3), 0.16 (d, 3, J_{CH} = 115, ZrCH_3). ^{13}C NMR of **6b$_1$** (126 MHz, 20 °C, C_6D_5Br): δ 47.83 (br, ZrCH_3), 45.74 (s, NCH_3). The ^{13}C-labeled complex {[N_2N(*CH_3)]Zr(#CH_3)}$^+$ was prepared from ^{13}C-labeled **1b** by the same procedure.

Line Shape Analyses. The line shape analysis in Figure 8a was carried out by considering an exchange between two sites with a population difference calculated according to the observed or extrapolated equilibrium constant and a bandwidth of 4 Hz.

The line shape analysis for [{[N_2NMe]Zr(CH_3)}$_2$(μ-CH_3)][B(C_6F_5)$_4$] was carried out (gNMR software) by modeling the two coalescing *o*-CH_3 resonances near 1.50 ppm in a spectrum in C_6D_5Br at 500 MHz. A bandwidth of 3 Hz was employed. The calculated values for k in s^{-1} (temperature T in K) are 12 (248.3), 25 (258.6), 70 (268.8), 180 (279.4), 400 (289.7), 810 (299.7), 1900 (309.3), 4100 (318.8), and 7000 (329.6). An Eyring plot yielded $\Delta H^{\ddagger}$ = 52.3 ± 1.3 kJ mol^{-1} and $\Delta S^{\ddagger}$ = −14 ± 5 J K^{-1} mol^{-1}.

Acknowledgment. We thank the Department of Energy (Contract No. DE-FG02-86ER13564) and Exxon Corp. for supporting this research. A.L.C. thanks The Ministerio de Educación y Cultura (Spain) for a postdoctoral fellowship and Dr. Jeff Simpson of the MIT Spectroscopy Laboratory for assistance with NMR techniques.

Supporting Information Available: Text giving experimental procedures, fully labeled ORTEP drawings, and tables giving crystal data and structure refinement details, atomic coordinates, bond lengths and angles, and anisotropic displacement parameters for [N_2NH]ZrMe_2, {[N_2NMe]ZrMe(ether)}[B(C_6F_5)$_4$], and [[N_2NMe]ZrMe}$_2$(μ-CH_3)][B(C_6F_5)$_4$]. This material is available free of charge via the Internet at http://pubs.acs.org. Supporting X-ray information for [N_2NMe]ZrMe_2 can be found in the preliminary communication.[4]

OM0004996